Reconstructing the geological history of the Lower Jurassic Jordan Formation: A comprehensive analysis and first record in the Mesa de San Pedro (Colombia), South America

Oscar Mauricio Castellanos-Alarcón[1], Carlos Alberto Ríos-Reyes[2*], Jorge Arley Meza-Ortíz[2]

[1]Facultad de Ciencias Básicas, Universidad de Pamplona, Autopista San Antonio, Villa del Rosario, Colombia. oscarmca@yahoo.es

[2]Escuela de Geología, Universidad Industrial de Santander, Cra 27 Cl 9, Bucaramanga, Colombia. carios@uis.edu.co; jorgearley.meza@gmail.com

[*]Corresponding author: carios@uis.edu.co

Abstract

This study presents the first-ever documentation of volcaniclastic rocks (tuffs) within the Jurassic Jordán Formation at the Mesa de San Pedro (Colombia). The lithostratigraphic sequence involves the pre-Devonian Mesa de San Pedro Phyllites, followed by the Jurassic Jordán Formation, characterized by an alternation of red to purplish mudstones, slightly sandy and micaceous very fine-grained sandstones, and the newly identified volcaniclastic rocks. This discovery holds significance as it sheds light on the environmental conditions during the fluvial-lacustrine sedimentation of the Jordán Formation, indicating syn-sedimentary volcanic activity during the Jurassic period. The Mesa de San Pedro, a remnant of an ancient structural plateau dissected by the Chicamocha River, unveils crucial lithological contacts and field relationships. The stratigraphic sequence, primarily consisting of the pre-Devonian Mesa de San Pedro Phyllites, the Jurassic Jordán Formation, and the Lower Cretaceous Los Santos Formation, is observed in the study area. Special attention is given to the occurrence of interbedded volcaniclastic rocks within the red layers previously misreported as the Girón Formation. This study corrects the misclassification and reports the Jordán Formation in the San Pedro Mesa for the first time. The thickness is approximately 95 m, comprising siltstones, very fine to fine-grained reddish-brown sandstones, and volcaniclastic rocks. The felsic explosive volcanic component is restricted in distribution, mainly concentrated in the morphostructure and adjacent areas.

Keywords: Santander Massif, San Pedro´s Phyllites, volcaniclastic rocks, tuffs, magmatism.

1. Introduction

During the Late Paleozoic and Early Mesozoic periods, the northwestern margin of South America (Gondwana) underwent significant geological transformations due to the convergence of the Farallón oceanic plate, resulting in the creation of the Panthalassa subduction zone along Pangaea's western margin (e.g., Mišković et al., 2009; Belica et al., 2017; Riel et al., 2018). The breakup of the Pangaea supercontinent was preceded by the emergence of extensional basins during the Triassic and Jurassic periods along the proto-Caribbean margin of northern South America, as well as in the area that now corresponds to the Gulf of Mexico (e.g., Pindell and Kennan, 2009). In Colombia, the Late Triassic to Early Jurassic interval is particularly noteworthy, marked by tectonic events such as the fragmentation of Pangaea and the initiation of ocean basin formation, leaving a lasting imprint on the geological landscape (Bayona et al., 2020). Various space-time models elucidate the geological processes during this period, including the formation of Jurassic intracontinental rifts, lateral migration of magmatic arcs, and the generation of magmatic arcs along the western margin of Gondwana (Cediel et al., 2003; Bayona et al., 2010; Cochrane et al., 2014; Spikings et al., 2015; Rodríguez et al., 2018; Nova et al., 2019). These models provide fundamental insights into the interplay between plutonism, volcanism, and sedimentation in northwestern South America. In the Colombian Andes, the Early Jurassic is marked by magmatism evidenced by belts of intrusive rocks and volcanic sequences in the Santander Massif, Central Cordillera, San Lucas Range, and Sierra Nevada de Santa Marta (e.g., Van der Lelij, 2016; Quandt et al., 2018; Shaw et al., 2019). The stratigraphy reveals thick successions of volcanic and volcaniclastic rocks interbedded with sedimentary rocks in various regions, including the Upper and Middle Magdalena Valley, San Lucas Range, Perijá Range, Sierra Nevada de Santa Marta, and the Guajira Peninsula (e.g., Maze, 1984; Clavijo et al., 2008; Leal-Mejía, 2011; Zuluaga et al., 2015; Rodríguez et al., 2016; Tschanz et al., 1974; Quandt et al., 2018). The Santander Massif, located in the northeastern part of Colombia, is characterized by a magmatic event with intrusive rocks from the Late Triassic to Early Jurassic (e.g., Goldsmith, et al.,1971; Ward, et al.,1973; Van der Lelij, 2016; Rodríguez, et al., 2020). The sedimentary record in the western foothills of the Santander Massif, represented by the Bocas and Jordan formations, provides a continuous record of lacustrine continental sedimentation with syn-sedimentary volcanic activity (Alarcón and Rodríguez, 2019). There is evidence of the occurrence of volcanic and volcaniclastic rocks in these lithostratigraphic units (e.g., Cediel, 1968; Ward et al., 1973; Ayala-Calvo et al., 2005; Toro-Toro et al., 2021). While the age of the Bocas Formation remains debated, with proposed Permian and Triassic ages, the Jordan Formation is assigned an Early Jurassic age based on U/Pb geochronology (Van der Lelij, 2016; Alarcón et al., 2020; Cohen et al., 2020). Several authors have reported the presence of volcanic rocks within the Jordan Formation, characterized by felsic tuffs of limited lateral continuity interbedded with red mudstones and sandstones (e.g., Cediel, 1968; Suárez and Díaz, 2016; Alarcón and Rodríguez, 2019). However, despite these regional insights, there is a lack of detailed petrographic and geochemical characterization of the volcaniclastic components within this formation, especially in localized settings such as the Mesa de San Pedro. This area represents a key window into the complex sedimentary-volcanic interactions during the Early Jurassic, a period characterized by simultaneous subduction and breakup processes across northwestern Gondwana, processes that are not fully understood in this region (Toro-Toro et al., 2021; Molina-Garza et al., 2021). Understanding the volcanic-sedimentary processes in this particular region is crucial, as it contributes to the broader knowledge of the tectonic and magmatic evolution of the northern Andes, with implications for analogous geological settings worldwide. This study focuses on outcrops of sedimentary rocks from the Jordan Formation in the Mesa de San Pedro, where thin layers of volcaniclastic rocks are prominent. By analyzing these rocks, we aim to address a critical gap in the understanding of local volcanic activity and sedimentation dynamics in the context of broader regional tectono-magmatic evolution. Given the complexity of the Early Jurassic geologic setting and the scarcity of similar studies in this area, this research offers new insights into the interactions between volcanic and sedimentary processes in a region of significant tectonic activity. The objective is to provide new petrographic and geochemical evidence from these volcanic tuffs in the Mesa de San Pedro area, thereby contributing to a better-defined and locally grounded understanding of the geological processes active during the Early Jurassic in this part of Colombia.

2. Geological setting

The Santander Massif, which is situated in the Eastern Cordillera of Colombia, holds a key position in the septentrional Andes, considering that it represents the junction between the NW–striking continuation of the Eastern Cordillera and the ENE-trending Mérida Andes in Venezuela (Fig. 1). According to Mann et al. (2006), it forms part of the Maracaibo Block, which is delineated by the Santa Marta–Bucaramanga and Oca strike–slip Fault Systems and the southwestern fold–and–thrust belt of the Mérida Andes. The geological constitution of the Santander Massif encompasses deformed and metamorphosed rocks, which have been tectonostratigraphically divided into three separate metamorphic units (Precambrian Bucaramanga Gneiss Complex, Pre-Devonian Silgará Formation, and Ordovician Orthogneiss), which represent the ancient rocks of this massif. These rocks were intruded by several igneous bodies, most of them of Triassic-Jurassic age and some of Paleozoic age. This massif has also been intruded by numerous igneous rocks, with the majority dating to the Triassic and Jurassic periods, while some can be traced back to the Paleozoic era (e.g., Goldsmith et al., 1971; Boinet et al., 1985; Mantilla et al., 2012; Zuluaga and López, 2019). These intrusions are acknowledged as integral components of the Santander Plutonic Complex, thought to be calc-alkaline crustal structures that were emplaced subsequent to the peak of metamorphism. Surrounding the central rock formations, sedimentary strata with ages ranging from the Devonian to the Tertiary period are found. The southwestern Santander Massif is significantly influenced by the Bucaramanga and Los Santos – Aratoca faults. The Bucaramanga Gneiss Complex, which represents the oldest unit of the igneous-metamorphic basement of the Santander Massif, outcrops towards the northwest as a sequence primarily composed of quartz-feldspathic biotitic and sillimanitic gneisses with intercalations of hornblende gneisses, quartzites, and amphibolites (e.g., Ureña and Zuluaga, 2011). These rocks attained high-temperature amphibolite facies metamorphic conditions. It is common to observe intense mylonitization in these rocks associated with the Bucaramanga Fault. Ríos et al. (2003) conducted a detailed study of the metapelitic sequence of the Silgará Formation that outcrops in this area, including isograd mapping and evaluation of metamorphic conditions. These rocks are essentially composed of bimicaceous schists with the presence of garnet, staurolite, and limited sillimanite, andalusite, and kyanite, along with phyllites and intercalations of quartzites, amphibolites, and calc-silicate rocks. These authors defined a metamorphic zonation ranging from the biotite zone to the sillimanite zone, indicating a low to high-temperature and medium-pressure Barrovian-type metamorphism. Nevertheless, Mantilla et al. (2016) defined a chlorite zone. The crystalline rocks are represented by the calc-alkaline intrusive rocks of the Mogotes Quartzmonzonite and the Pescadero Monzogranite. Recent research by Rodríguez et al. (2019) has established that these intrusive igneous rocks exhibit a chronological spectrum extending from the Late Triassic to the Early Jurassic, with estimated ages falling within the range of approximately 214.5 to 184.1 Ma. Concordantly overlying this igneous-metamorphic basement are red beds from the Bocas, Jordán, and Girón formations, to which ages ranging from the Late Triassic to the Early Cretaceous have been assigned (e.g., Pons, 1982; Horton et al., 2015; Alarcón et al., 2020; Toro-Toro et al., 2021; Jiménez et al., 2021). A sequence of Cretaceous sedimentary rocks unconformably overlies this succession of red beds. The site of interest in the present study is situated in the region of the Mesa de San Pedro (Colombia), Fig. 1. The metamorphic basement is made up of a very low-grade of metamorphism sequence of gray chloritic phyllites, with plane-parallel foliation, interspersed with metasandstones and metamudstones with weak foliation that outcrop towards the base of this morphostructure. Mantilla et al. (2016) have named this metamorphic sequence as the “San Pedro´s Phyllites”, assigning it a maximum stratigraphic age of the Middle Ordovician, to refer to very low-grade metamorphic rocks composed essentially of metapsammites and metapelites, and possibly locally metavolcaniclastic rocks (?), to which they assigned the peak of metamorphism with the Famatinian orogenic event (of Silurian age). However, we consider that, although the ages of detrital zircons can provide valuable information, especially in reconstructing the sedimentary history of a region, they are not sufficient to divide metamorphic units or directly date metamorphism. It is essential to combine this information with other geological data and use a variety of dating techniques to obtain an accurate picture of the geological history of a region. Therefore, in this study, we adopt the name San Pedro´s Phyllites to refer to a sequence of lower-grade metamorphic rocks recorded in the Silgará Formation, whose sedimentary protoliths were tectonically transported to shallower structural levels of the Earth's crust, developing metamorphic zones of biotite (Ríos et al., 2003) and probably chlorite (Mantilla et al., 2016). The Jordan Formation´s red beds were unconformably deposited on these basement rocks, which are characterized by an alternation of red to purplish mudstones, locally fissile, slightly sandy and micaceous, very fine-grained sandstones, and very thin layers of sandy tuffs and tuffs of reddish color. Rhyolitic rocks are also sparsely distributed along the roads leading to the El Guásimo and Los Totumos sidewalks. The Lower Cretaceous Los Santos Formation, overlying the Jordan Formation, consists of conglomerates and conglomeratic sandstones of its lower member towards the base, and medium-grain sandstones of cream-white color, with mainly yellowish tones, in competent layers of tabular geometry with plane-parallel stratification, towards the top. Along the carriageway that leads to the Los Totumos sidewalk, Castellanos and Ríos (2008) report the occurrence of a petrified wood trunk, approximately 180 cm long and 40 cm in diameter, petrified wood in strata of the Girón Formation. According to these authors, the original wood trunk underwent pseudomorphism by silica, showing evidence of dissolution, replacement, and differential shortening processes as a product of diagenesis and fossilization. However, since its replacement has been complete, it is difficult to carry out a taxonomic classification of this fossil specimen in order to establish its significance as a paleoclimatic indicator. This finding is of great importance because fossil woods from the Triassic and Cretaceous periods are known in South America, although their record during the Jurassic is scarce (Torres and Philippe, 2002). Here, geomorphological and tectonic features of the Aratoca Fault are also observed, which constitutes a dextral strike tectonic structure with an inverse component, highly verticalized and with a dip plane to the NE (Rojas-Parra and Gómez-Isidro, 2007). In this study, particular emphasis will be placed on the sequence of the Jordan Formation, as it holds significant relevance for the present investigation. It exhibits distinctive lithological characteristics and sedimentary features that provide valuable insights into the depositional processes and paleoenvironmental conditions of the region. By focusing on this particular sequence, we aim to document and interpret volcanic-sedimentary interactions that have not been previously characterized in the Mesa de San Pedro region. This study contributes to filling a gap in the regional stratigraphic and volcanic record of the Lower Jurassic in the northern Andes, thereby refining the geological history of this key tectonic and magmatic period in Colombia.

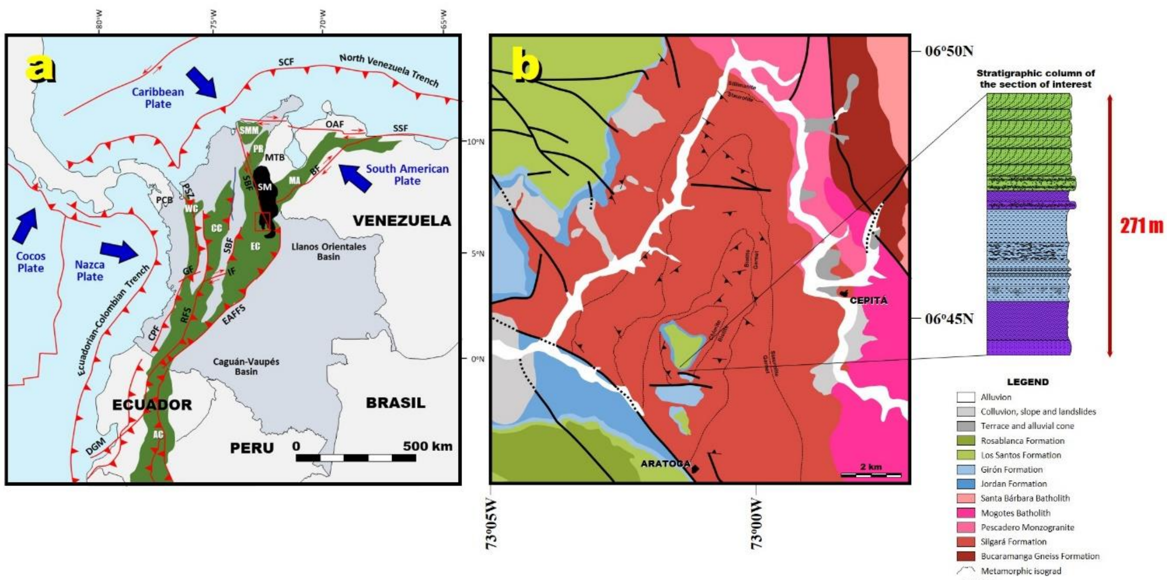

Fig. 1. (a) Major tectonic and structural features of the NW margin South America (modified from Colmenares and Zoback, 2003). SCF, Southern Caribbean Marginal Fault; SMM, Santa Marta Massif; SM, Santander Massif; PR, Perijá Range; MA, Merida Andes; AC, Andes Cordillera; OAF, Oca-Ancón Fault; SSF, San Sebastián Fault System; SBF, Santa Marta-Bucaramanga Fault; RFS, Romeral Fault System; SBF, Salina-Bituima Fault;

BF, Boconó Fault; PSZ, Panamá suture zone; GF, Garrapatas Fault; IF, Ibagué Fault; CPF, Cauca-Patía Fault; MTB, Maracaibo Triangular Block; PCB, Panamá-Chocó Block; EC, Eastern Cordillera; CC, Central Cordillera; WC, Western Cordillera; EAFFS, Eastern Andean Front Fault System; DGM, Dolores–Guayaquil Megashear. (b) Generalized geological map (modified from Ward et al., 1973; Ríos et al., 2003; Mantilla et al., 2016), showing the location of the stratigraphic sequence of interest in this study.

3. Materials and methods

3.1. Fieldwork

Recently, a fieldwork in the studied area, allowed a recognition of the outcropping lithologies with special emphasis on the contact between the Jordan Formation and adjacent geological units in the Mesa de San Pedro and the El Guásimo and Los Totumos sidewalks. Twenty-five (25) rock samples were collected for petrographic and geochemical analyses from approximately six (6) outcrops of the Jordan Formation, making emphasize in the sector of the Mesa de San Pedro, where it had previously been mapped as the Girón Formation, and the decision to conduct geochemical analyses on only two (2) rock samples is justified as follows. They were carefully chosen to accurately represent the geological diversity within the Jordan Formation. Outcrops were specifically selected to serve as representative examples of the formation's composition and geological characteristics in the study area. Geochemical analyses demand substantial resources, including both time and budget constraints. Therefore, the decision was made to analyze a restricted number of samples in order to optimize the utilization of the available resources. The samples were gathered from regions of the Jordan Formation that held particular significance for the study's objectives.

This includes areas with unique geological features, evidence of specific processes, or transitional zones between distinct geological units. Rather than conducting analyses on all collected samples, a selective sampling strategy was employed. This approach allowed for concentrated attention on samples that showed the most promise in terms of providing pertinent and valuable information. Geochemical analyses on a subset of samples can yield preliminary findings that help shape the study's direction. This is particularly useful in deciding whether further analyses on a larger number of samples are warranted.

3.2. Samples preparation and analytical methods

A macroscopic characterization of hand samples of rock was carried out in order to determine those of greatest interest for their preparation and investigation by different analytical techniques. Preparation of 5 polished thin sections of rocks for petrographic analysis was performed by transmitted light microscopy, using a trinocular Olympus BX-51, which helps to identify textural and microstructural features of the analyzed rocks. The geochemistry of major and minor elements in whole-rock samples was conducted in the ALS Minerals laboratories in Colombia. It was performed using Inductively Coupled Plasma Mass Spectrometry (ICP-MS) following the specified standards and parameters for sample preparation and analytical procedures: WEI21 (weighing), CRU-QC (crushing with quality control test), PUL-QC (pulverization with quality control test), CRU-31 (fine crushing - 70% < 2 mm), PUL-31 (fine crushing - 85% < 75 µm), ME-4ACD81 (basic metals - digestion with four acids), ICP-AES, ME-ICP06 (determination of major, minor, trace and rare-earth elements using mass spectrometry), and OA-GRA05 (loss on ignition at 1000°C). Data processing was carried out using Geochemical Data ToolKit (GCDKit) version 3.00 developed by Janoušek et al. (2006).

4. Lithostratigraphy and field relationships

The Mesa de San Pedro (Fig. 2) is a remnant of an ancient structural plateau that was dissected by the Chicamocha River and its tributaries. Along an unpaved road leading from the Parador Los Morenos on the national highway connecting the cities of Bucaramanga and Bogotá (capital of the Republic of Colombia) to the top of the Mesa de San Pedro, two significant lithological contacts and field relationships are encountered between the pre-Devonian San Pedro's Phyllites, the Lower Jurassic Jordan Formation, and the Lower Cretaceous Los Santos Formation, as described below. It is essential to note that it is not uncommon to find this Lower Jurassic – Lower Cretaceous stratigraphic interval resting in erosive unconformity on the oldest rocks of the Santander Massif. In this area, the stratigraphy is significantly affected by satellite faults associated with the Aratoca Fault, which cause a complex juxtaposition of older and younger units. These faulting events, and the tectonic reworking they caused, may explain the unusual stratigraphic relationship where Paleozoic rocks, such as the San Pedro's Phyllites, are located in the middle of the Lower Jurassic and Lower Cretaceous sequences. The occurrence of the San Pedro's Phyllites in this context suggests a tectonically disturbed zone, possibly the result of faulting or erosional processes that have uplifted and exposed older rocks in the midst of younger sedimentary layers. The boundary between the Paleozoic San Pedro's Phyllites and the younger formations could be the result of an angular unconformity, where the older units were displaced due to tectonic movements associated with the regional fault system. Additionally, the younger rocks (the Jordan and Los Santos formations) could represent sedimentary sequences that were deposited over the uplifted Paleozoic units, possibly incorporating fragments or reworked materials from these older layers. This scenario is consistent with the idea of incised valleys or tectonic scarp erosion, which could have contributed to the incorporation of these older rocks into younger depositional environments. Furthermore, the boundaries between these units should be considered in the context of potential erosional unconformities and tectonic reworking, rather than simple stratigraphic deposition. These complex field relationships suggest that the geological history of the area involves substantial tectonic deformation, with the younger rocks resting unconformably on older units, likely due to faulting and subsequent erosion. Based on the results derived from the volcanosedimentary sequence of red beds exposed in the Mesa de San Pedro area and their stratigraphic position in relation to the one documented by Alarcón et al. (2020) in the Jordan Formation's type section in the Mesa de Los Santos, we propose, for the first time, the identification of this geological unit instead of the Girón Formation, as previously indicated in regional mapping (Jaramillo et al., 1969). Traditionally, in this remnant of an ancient structural plateau, it had been referred to as a thin sedimentary sequence of red beds belonging to the Girón Formation. This conclusion is based on the fact that only in the Bocas and Jordan formations have reported the presence of volcaniclastic rocks, while the Girón Formation lacks them. Fig. 3 illustrates a generalized stratigraphic column along the road leading from Parador Los Morenos to the top of the Mesa de San Pedro. The observed levels in the mentioned stratigraphic sequence are shown in Fig. 4 and described below.

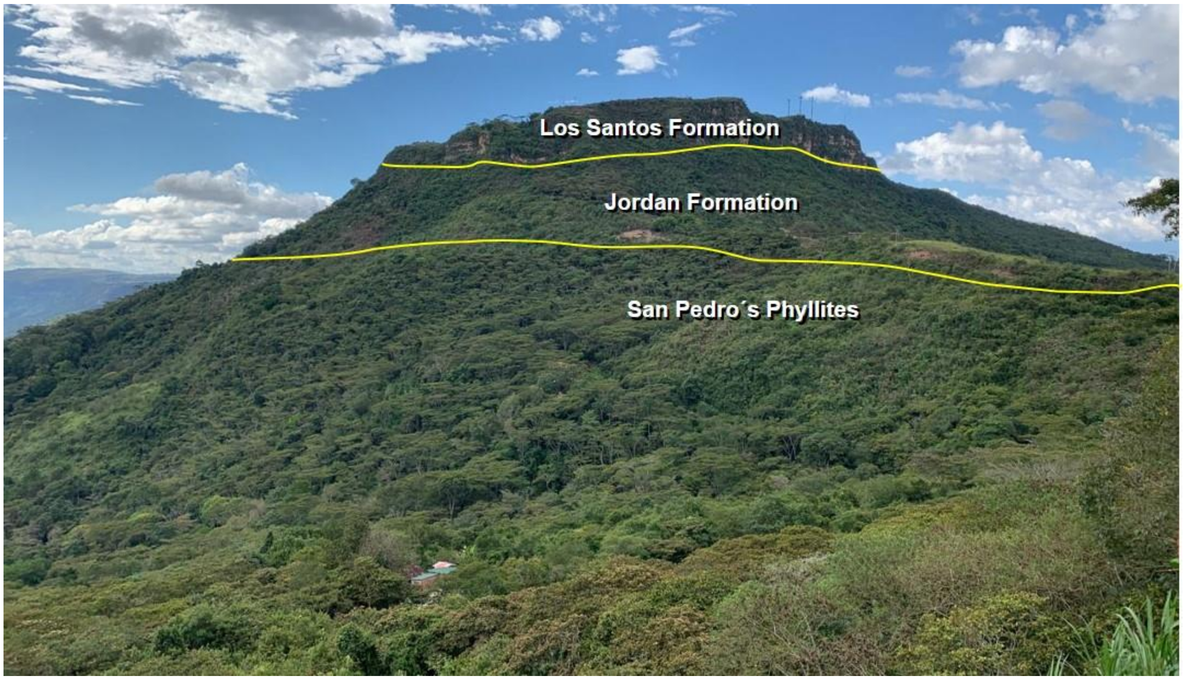

Fig. 2. Landscape of the Mesa de San Pedro, showing the lithostratigrafic sequence.

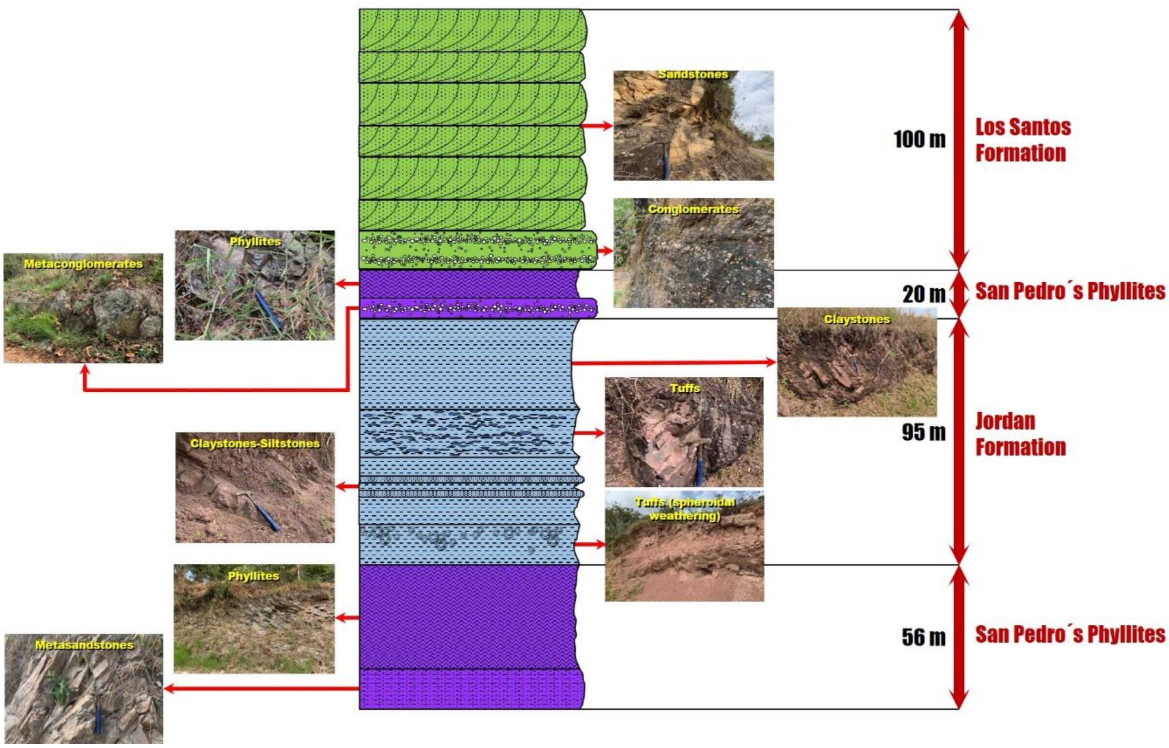

Fig. 3. Generalized stratigraphic column uplifted along the road leading from Parador Los Morenos to the top of the Mesa de San Pedro.

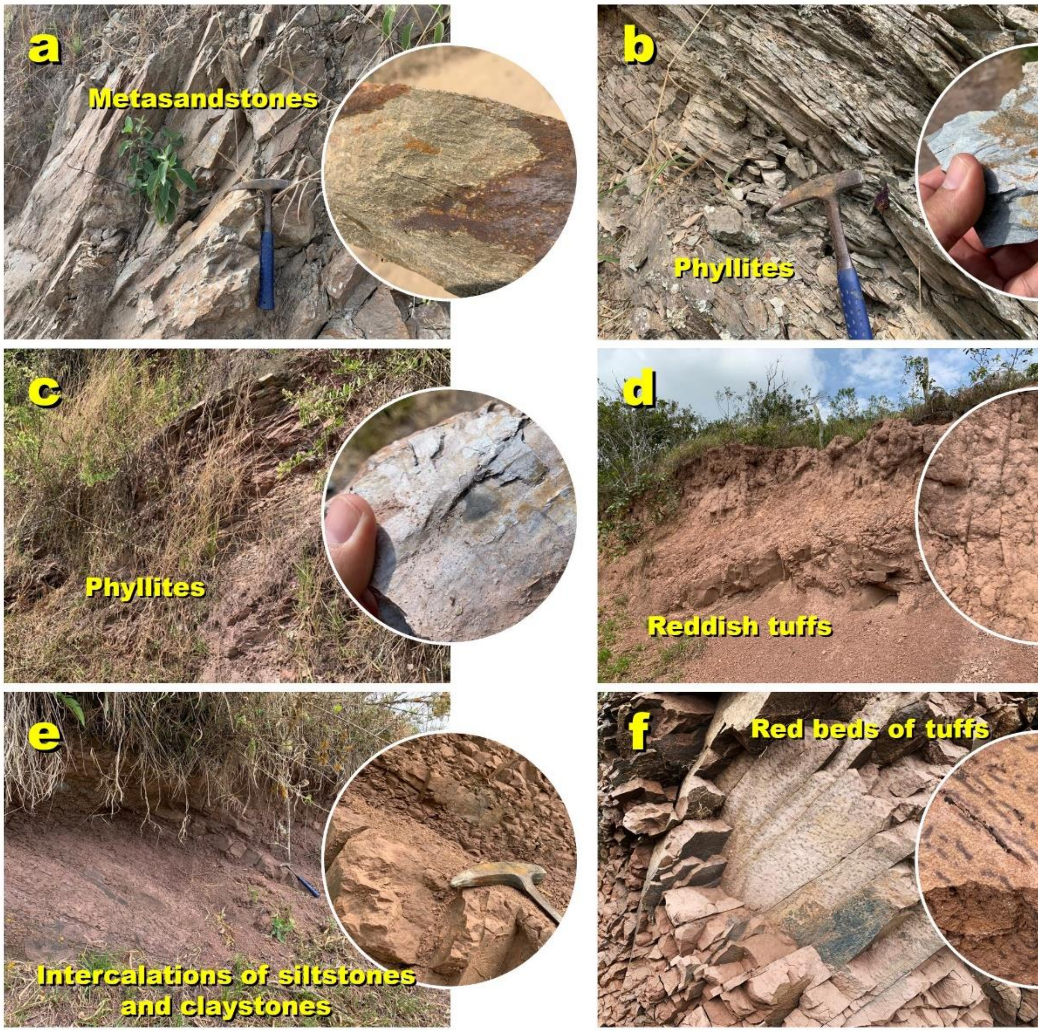

Fig. 4. Field occurrence of the Mesa de San Pedro Phyllites and volcaniclastic rocks of the Jordán Formation that outcrop in the Mesa de San Pedro.

4.1. San Pedro's Phyllites

At the base of the Mesa de San Pedro, there is a very low-grade metapelitic sequence of the Paleozoic San Pedro's Phyllites. Ascending stratigraphically, it is characterized by a predominance of intercalations of metasandstones (Fig. 4a) and gray chloritic phyllites (Fig. 4b) at km 0+000 (located at the Parador Los Morenos, where there is an entrance gate to the road that leads to the top of the Mesa de San Pedro), and gray-green phyllites (Fig. 4c) at km

0+085. These rocks display a planar-parallel metamorphic foliation with moderate to strong folding, and a silky appearance is notable on their foliation surface. The upper contact between the San Pedro's Phyllites and the overlying Jordan Formation is marked by a clear discordant surface at km 0+100.

4.2. Jordan Formation

At km 0+100, the Jordan Formation begins with a reddish tuff level, which displays tabular geometry and planar-parallel stratification, intense fracturing, and spheroidal weathering (Fig. 4d). At approximately km 0+275, there is a layer of red beds (Fig. 4e), characterized by the presence of intercalations of mudstones and claystones (?), which exhibit a tabular geometry and planar-parallel stratification, as well as fissility, particularly in the claystones. At km 0+300, a layer of red beds of tuffs is observed, displaying vesicular to amygdaloidal structures in its interior, as well as angular lithic clasts (Fig. 4f). Above this layer, planar-parallel bedded red mudstones are observed at km 0+320. The Jordan Formation rests unconformably upon the San Pedro's Phyllites and is underlain by the Los Santos Formation through an angular unconformity.

Fig. 5 shows the sampling localities and geographic coordinates of the studied volcaniclastic rocks of the Jurassic Jordan Formation. The bottom of the sequence of interest of the Jurassic Jordan Formation consists of tuffs, which develop spheroidal weathering (Fig. 6a). Fig. 6b illustrates the occurrence of volcaniclastic rocks (sandy tuffs and tuffs) with plane-parallel bedding on a millimeter scale, which show a high-angle fracturing with the bedding planes, as well as a nodular appearance in some sectors. Volcaniclastic rocks (sandy tuffs) with discrete stratification and mottled structure are shown in Fig. 6c. The top of this sequence shows interbedded tuffs into red to purplish mudstones, locally fissile, slightly sandy and micaceous, and very fine-grained sandstones of reddish color (Fig. 6d), which show a tabular geometry, plane-parallel bedding and jointing perpendicular to the bedding planes.

Sample No.	Geological unit	Lithology	Geographical coordinates		Petrography analysis	Geochemical analysis
			North	West		
TGA-1	Jordán Formation	Volcaniclastic rock	6.722518°	-73.019527°	Crystal tuff	X
TGA-2	Jordán Formation	Volcaniclastic rock	6.724099°	-73.020331°	Crystal tuff	
TGA-3	Jordán Formation	Volcaniclastic rock	6.724024°	-73.020253°	Vitreous tuff	X
TGA-4	Jordán Formation	Volcaniclastic rock	6.723749°	-73.020264°	Vitreous tuff	

Fig. 5. Google Earth satellite image showing the sampling localities and geographic coordinates of the investigated volcaniclastic rocks.

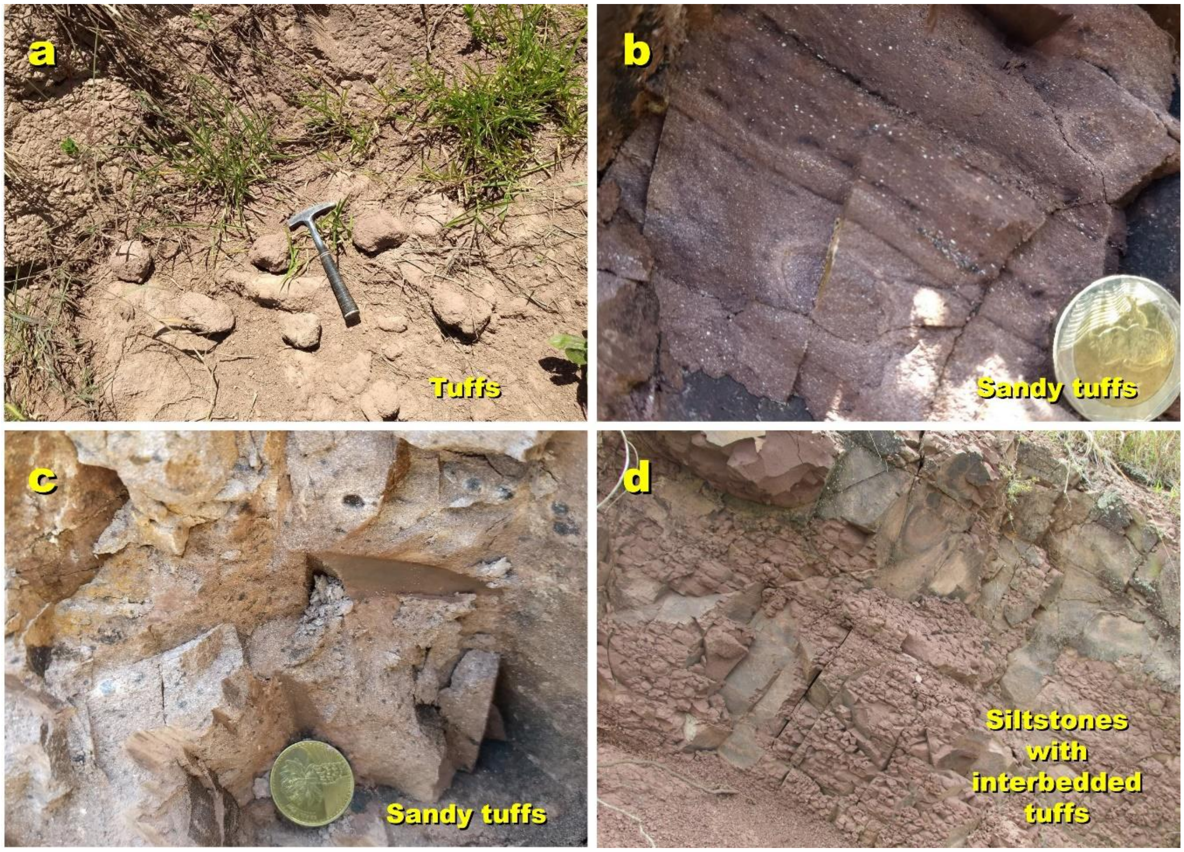

Fig. 6. Outcrops of the Jordan Formation. (a) Tuffs developing spheroidal weathering. (b)-(c) Volcaniclastic rocks (sandy tuffs). (d) Interbedded tuffs into red to violaceous mudstones.

The occurrence of the Jordan Formation in the Mesa de San Pedro is reported here for the first time, with an approximate thickness of about 95 m, characterized by monotonous intercalations of mudstones, very fine to fine-grained reddish-brown sandstones, and, to a lesser extent, volcaniclastic rocks (Fig. 7). The felsic volcanic component within the Jordan Formation is limited in extent, with its distribution being relatively small and primarily concentrated in this morphostructure and adjacent areas.

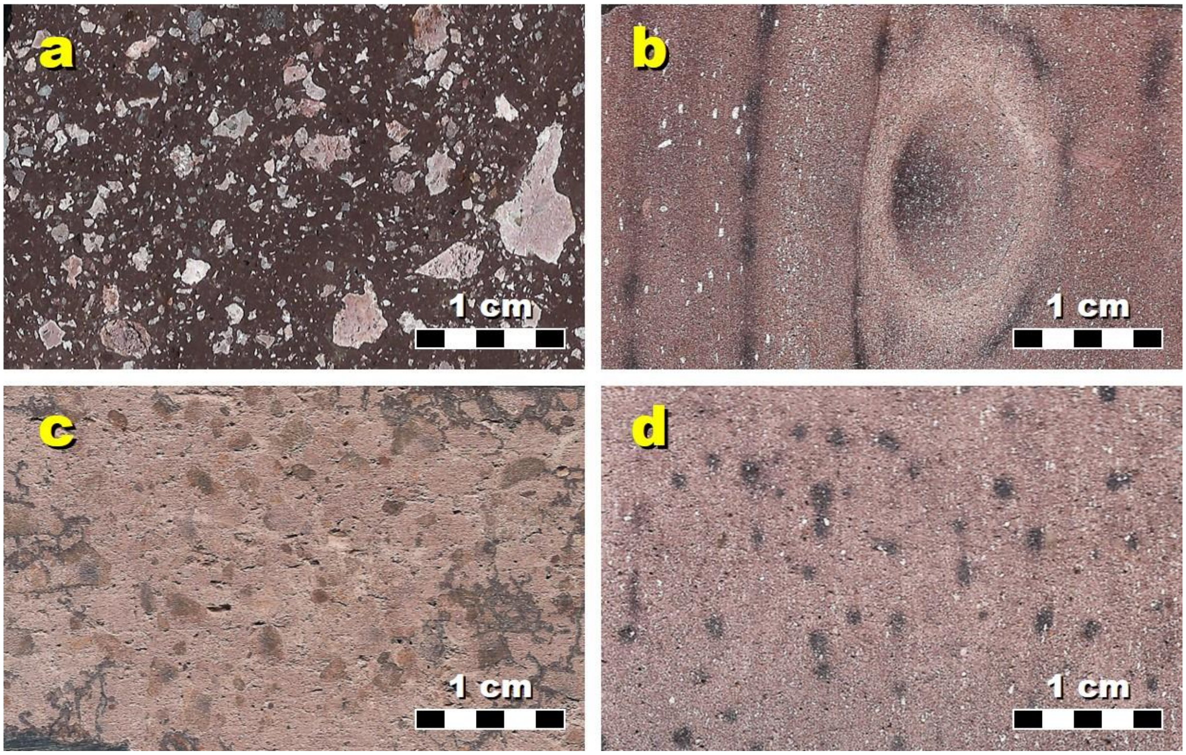

Fig. 7. Polished sections of the volcaniclastic rocks of the Jordán Formation and the sedimentary rocks of the Los Santos Formation that outcrop in the Mesa de San Pedro.

4.3. Los Santos Formation

At km 0+375, there is a contact between metaconglomerates(?) of the San Pedro's Phyllites and the Jordan Formation's red beds as shown in Fig. 8a, which marks the beginning of the sedimentary sequence of the Los Santos Formation. At km 0+575, the basal conglomerates of the Lower Cretaceous Los Santos Formation overlie gray to dark gray phyllites (Fig. 8b). These conglomerates occur between km 0+775 and 0+805 (Figs. 8c-8d). However, the Los Santos Formation consists of conglomerates and conglomeratic sandstones in its lower member toward the base. At km 1+000, these conglomerates are conformably overlain by medium-grain sandstones of cream-white color, primarily with yellowish to orangish tones in competent layers with tabular geometry and planar-parallel stratification (Fig. 8e). At km

1+200, these sandstones exhibit a mottled appearance with green to violet hues (Fig. 8f). The top of this sedimentary unit is located at km 1+300, where orange-colored sandstones predominate, displaying a tabular to lenticular geometry.

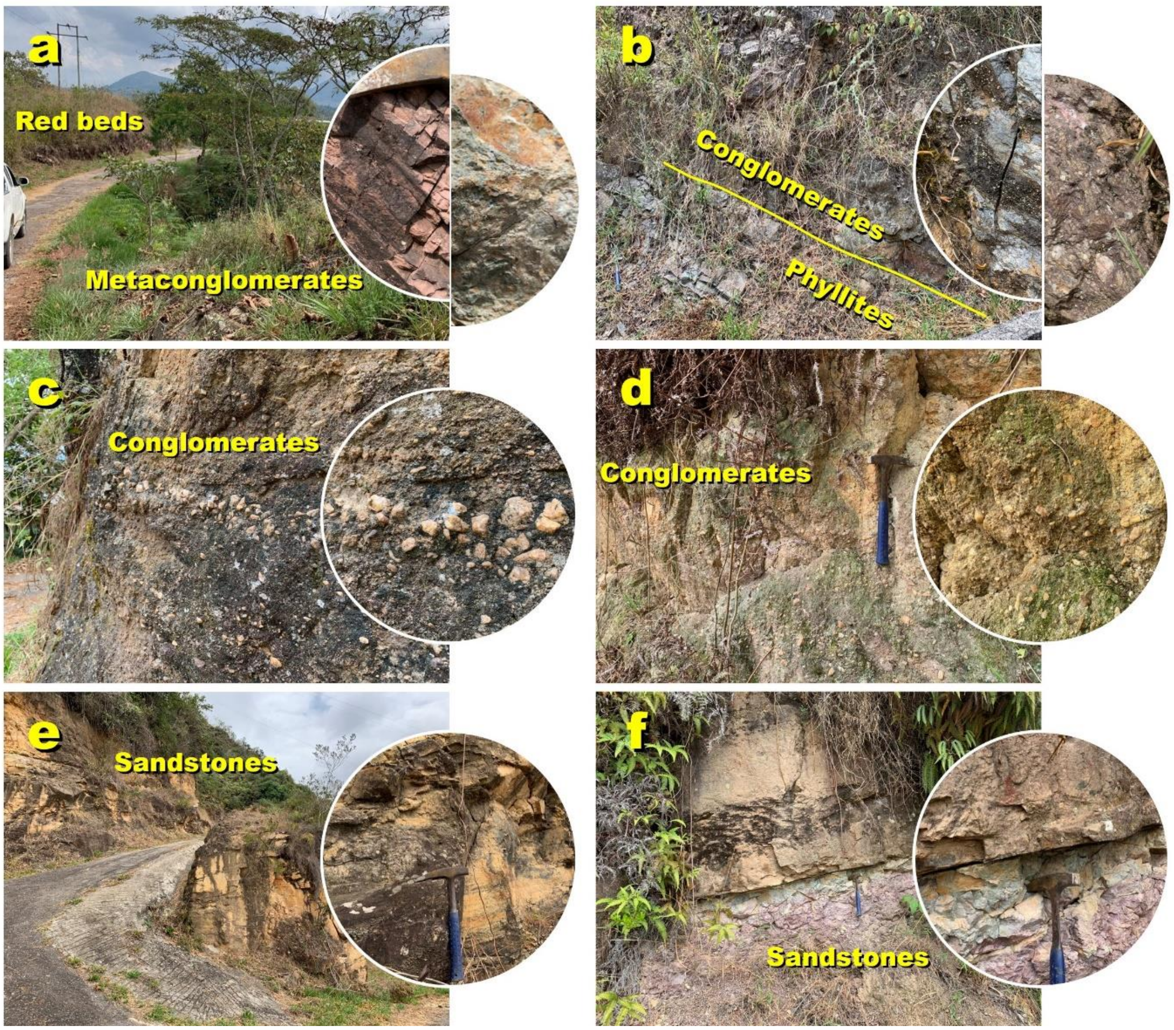

Fig. 8. Main structural and textural features of the volcaniclastic rocks of the Jurassic Jordan Formation. (a) TGA-1. (b) TGA-2. (c) TGA-3. (d) TGA-4.

5. Petrography

The volcaniclastic rocks examined in this study are identified as rhyolitic tuffs, classified as lithic, crystal-rich, and vitric. These tuffs exhibit a fragmental texture, containing varying amounts of crystal and lithic fragments. The matrix ranges from vitric to cryptocrystalline due to devitrification. A flow texture is evident in the matrix, occasionally featuring flame structures, which is characteristic of the eutaxitic texture seen in ignimbrites. Juvenile crystal fragments primarily consist of K-feldspar, plagioclase, quartz, and, to a lesser extent, muscovite, biotite, and opaque minerals (magnetite). Juvenile lithic fragments are mainly felsic volcanic rocks (rhyolitic tuffs) and, to a lesser extent, accidental metamorphic lithics such as phyllites and metasandstones, which resemble the lithologies found in the San Pedro Phyllites. Although this petrographic analysis was based on a limited number of samples, it is important to highlight that the volcaniclastic sequence studied here represents an exceptionally rare and thin stratigraphic exposure within the Santander Massif. The restricted lateral extent and localized preservation of the outcrop inherently constrained our ability to collect additional material.

Fig. 7 presents photographs of polished sections of the volcaniclastic rocks from the Jordan Formation, highlighting their key structural and textural features. Figs. 7a-7b show a tuff that has undergone spheroidal weathering, with its fragmentary appearance evident in both the outer and inner parts. Fig. 7c depicts a sandy tuff with plane-parallel bedding at the millimeter scale and a nodular appearance in some areas. Fig. 7d shows a sandy tuff with discrete stratification and a mottled structure.

Sample TGA-1 (Fig. 9) consists of an ash and lapilli tuff with a slightly altered vitreous matrix that exhibits a dense and solid structure. Mineralogically, it is composed of quartz (24%), plagioclase (3%), biotite (1%), volcanic glass (20%), rock fragments (4%), and matrix (48%). According to Schmid's (1981) classification based on component types, it is classified as a crystal-rich tuff. In some areas, incipient pseudo-lamination is observed. The vitreous matrix composition cannot be clearly distinguished petrographically due to the oxide patinas, such as limonite, which cover the clay aggregates and mask the interference colors, giving it an isotropic character. A high content of pyroclasts and epiclasts is identified, primarily composed of volcanic glass with localized alteration to clay minerals. Additionally, anhedral quartz and feldspar epiclasts are present. The quartz grains range from coarse to fine and are angular to subangular, while the feldspar grains, which are smaller, range from coarse to fine and exhibit predominantly subhedral to euhedral forms. The rock shows low grain selection, indicating a wide dispersion in grain size. The relationship between the pyroclasts and the matrix is not clear, suggesting a possible depositional origin rather than a pyroclastic one. However, cathodoluminescence studies are suggested to clarify the origin of the quartz and the matrix containing the rock fragments. The low anisotropy of the minerals in the matrix may be due to their volcanic origin. Nevertheless, field relationships suggest a more consolidated volcaniclastic deposition origin.

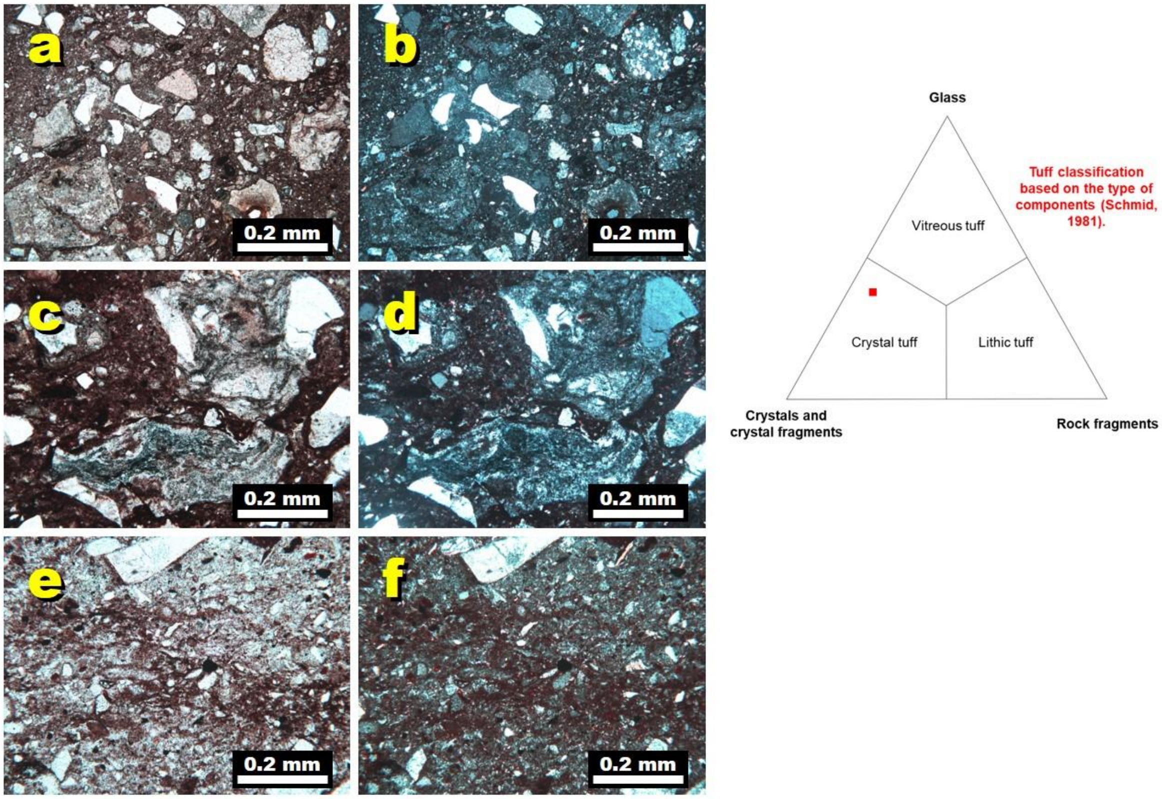

Fig. 9. Left, thin-section photomicrographs in PPL and XPL showing the petrographical features of the sample TGA-1 (ash and lapilli tuff) in the Jordan Formation. Right, tuff classification based on the type of components by Schmid (1981).

Sample TGA-2 (Fig. 10) corresponds to a consolidated tuff composed of very fine ash and dust with a vitreous matrix altered to clay minerals, giving it a dense appearance and a laminated structure. Mineralogically, it is composed of quartz (12.5%), plagioclase (5%), potassium feldspar (2%), biotite (0.5%), vitreous fragments (10%), and matrix (70%). Following Schmid's (1981) classification, it is a crystal-rich tuff. Locally, incipient planar-parallel lamination is observed. The vitreous matrix is partially altered to clay minerals, which cannot be differentiated petrographically due to the presence of oxide patinas, such as limonite, that cover the clay aggregates. Epiclasts of quartz and feldspar with morphological and grain size variations are observed. The quartz grains are angular to subangular, mostly subrounded, and range in size from silt to very fine sand. Notably, some subrounded quartz grains exhibit internal inclusions. The feldspar grains are similar in size to the ash and tend to be larger than the quartz epiclasts, mostly exhibiting subhedral to euhedral forms.

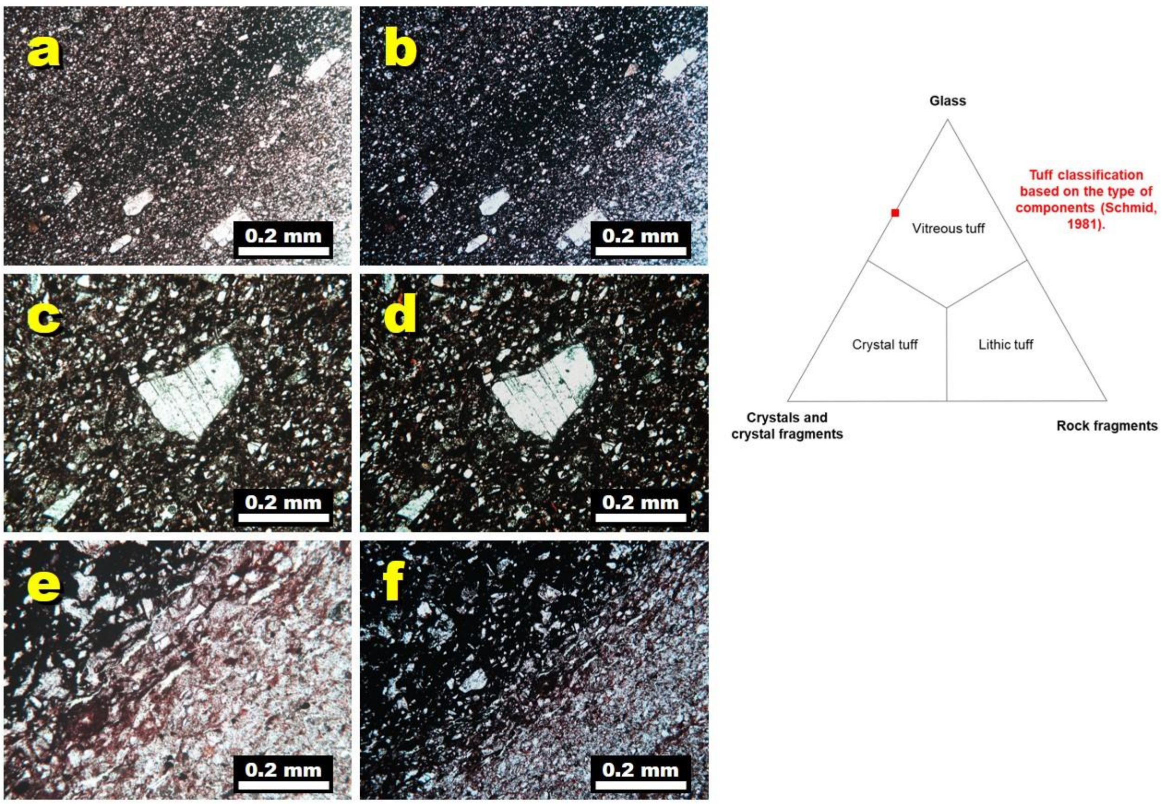

Fig. 10. Left, thin-section photomicrographs in PPL and XPL showing the petrographical features of the sample TGA-2 (consolidated tuff) in the Jordan Formation. Right, tuff classification based on the type of components by Schmid (1981).

Sample TGA-3 (Fig. 11) corresponds to a tuff composed of fine ash and dust, with a slightly altered vitreous matrix that is dense and solid. Mineralogically, it consists of clays (14%), quartz (6%), volcanic glass (15%), and matrix (65%). According to Schmid's (1981) classification, it is a crystal-rich tuff. Incipient pseudolamination is locally observed. The vitreous matrix composition is indistinguishable petrographically due to oxide patinas, such as limonite, which cover the clay aggregates and give it an isotropic character. The tuff contains a high proportion of pyroclasts and anhedral epiclasts of quartz and feldspar. The quartz grains are angular to subangular, ranging in size from very fine to silt, with some subrounded forms present. These grains are generally smaller than the feldspar grains, which range from medium to coarse sand and predominantly exhibit subhedral to euhedral shapes. Grain selection within the rock is low, indicating a high degree of grain size dispersion. The relationship between the pyroclasts and the matrix remains unclear. Initially, a depositional origin rather than a pyroclastic one can be inferred, but cathodoluminescence studies are recommended to determine the origin of the quartz and matrix. The observed relationships in the field suggest a consolidated volcaniclastic deposit origin.

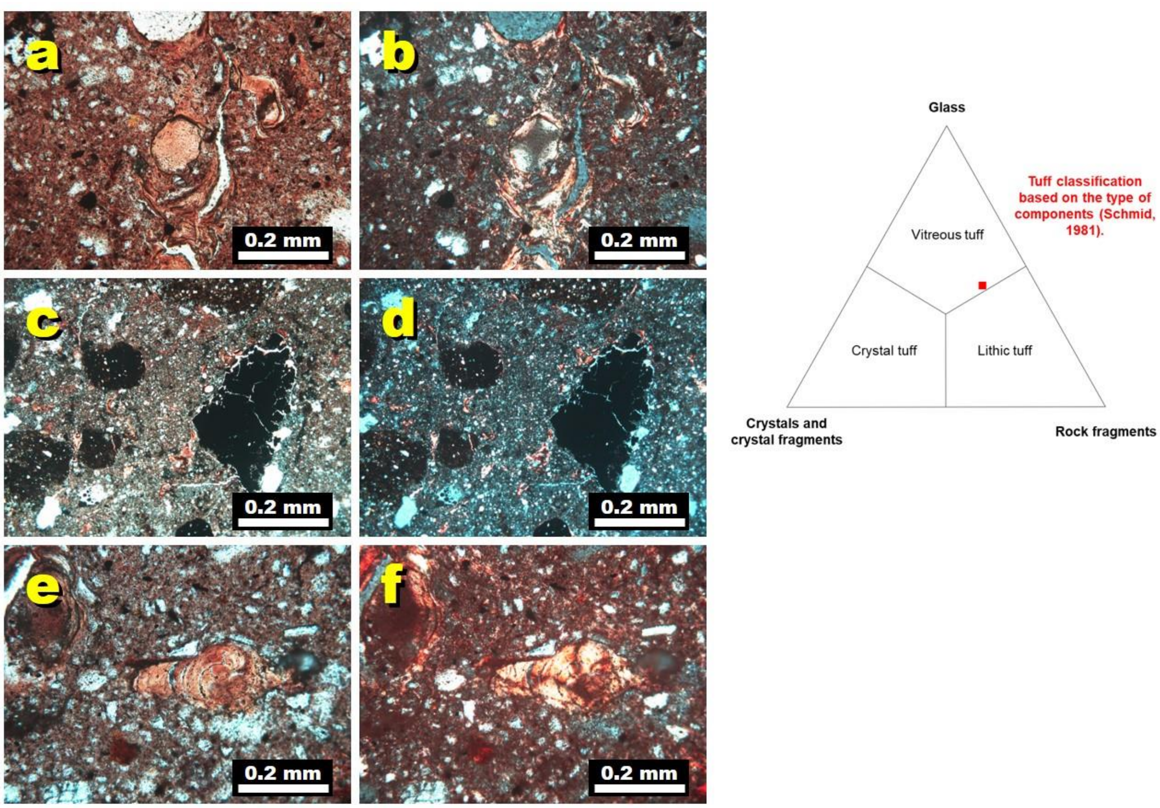

Fig. 11. Left, thin-section photomicrographs in PPL and XPL showing the petrographical features of the sample TGA-3 (fine ash and dust tuff) in the Jordan Formation. Right, tuff classification based on the type of components by Schmid (1981).

Sample TGA-4 (Fig. 12) is a tuff composed of ash and lapilli, with a vitreous matrix slightly altered by clays, resulting in a dense appearance and solid structure. Mineralogically, it consists of quartz (14%), plagioclase (10%), potassium feldspar (4%), and matrix (72%). Following Schmid's (1981) classification, it is a crystal-rich tuff. Incipient pseudolamination is occasionally observed. The vitreous matrix is difficult to distinguish petrographically due to the presence of an oxide patina, such as limonite, covering the clay aggregates, which imparts an isotropic character. The sample contains a significant amount of pumice and epiclasts, primarily consisting of ash to lapilli-sized quartz and feldspar crystals. The quartz grains range in size from medium to very fine sand and silt, mostly angular to subangular, though some subrounded grains are present. The feldspar grains are generally larger than the quartz grains, ranging from medium to coarse sand and exhibiting subhedral to euhedral forms. Grain selection is low, indicating high dispersion in grain size. The relationship between the pumice and matrix is unclear. At first glance, a depositional origin is suggested over a pyroclastic one, but cathodoluminescence studies are recommended to determine the origin of the quartz and matrix. The relationships observed in the field more clearly suggest a consolidated volcaniclastic deposition origin.

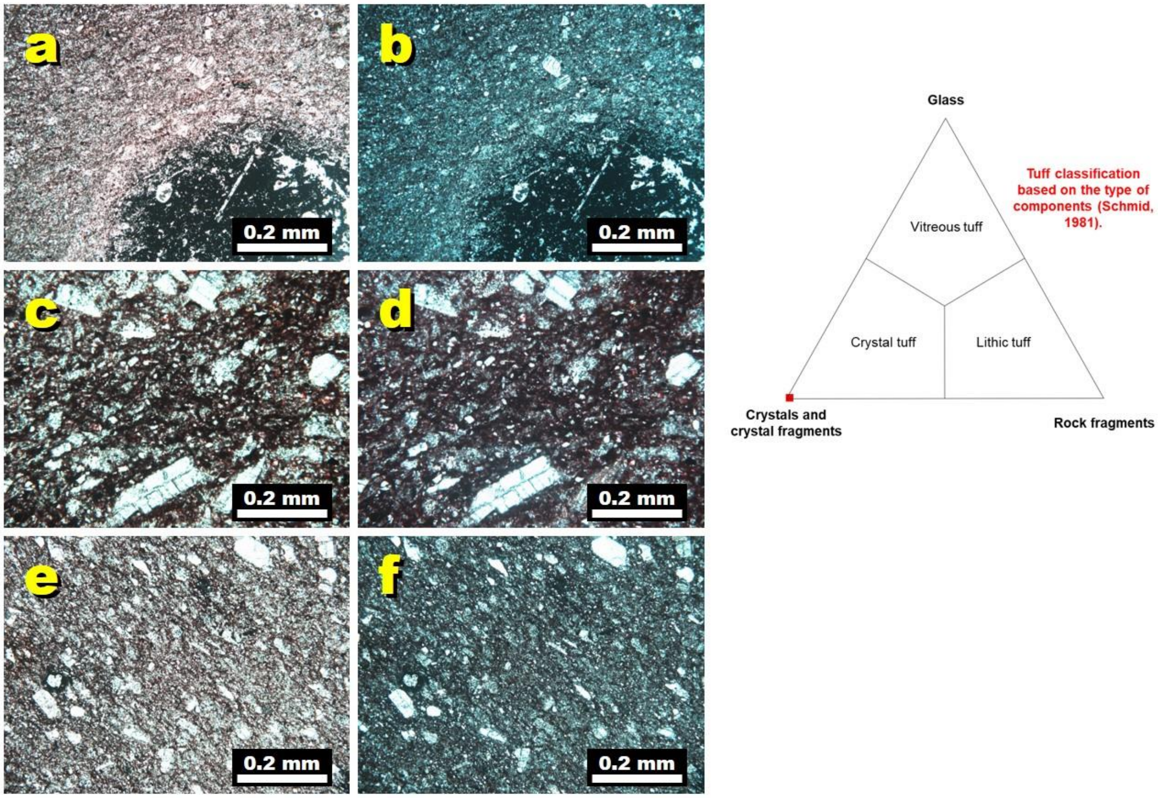

Fig. 12. Left, thin-section photomicrographs in PPL and XPL showing the petrographical features of the sample TGA-4 (ash and lapilli tuff) in the Jordan Formation. Right, tuff classification based on the type of components by Schmid (1981).

The petrographic study of the volcaniclastic rocks in the Jordan Formation provides valuable insights into the understanding of volcaniclastic rock types, mineralogical components, textures, and depositional history. These findings contribute to a global understanding of similar geological formations and volcaniclastic deposits, offering a useful reference for researchers and geologists worldwide. In this context, the petrographic results played a critical role in guiding the selection of samples for geochemical analyses. Given the exceptional nature of the exposure and the lack of comparable stratigraphic sections in the vicinity, this study should be seen as a preliminary but significant contribution toward the broader understanding of Lower Jurassic volcanic processes in the Santander Massif.

6. Whole-rock geochemistry

Whole-rock major, minor, trace and rare-earth element data (Table 1) were performed to characterize the volcaniclastic rocks from the Lower Jurassic Jordan Formation at the Mesa de San Pedro, which was guided by the selection of two samples based on petrographic criteria, with the overarching aim of shedding light on the primary genetic characteristics of these rocks. Although only two samples (TGA-1 and TGA-3) were selected for geochemical analysis, this decision was informed by detailed petrographic work and driven by the inherent limitations of the outcrop. The volcaniclastic sequence is extremely thin and geographically restricted, precluding the possibility of a broader sampling strategy. Furthermore, due to analytical and logistical limitations during the course of the research, complementary techniques such as isotope geochemistry or cathodoluminescence imaging could not be implemented, despite their acknowledged value for deciphering diagenetic and magmatic histories. These remain as important avenues for future research.

Table 1. Major oxides, trace, and rare earth element analyses of representative samples from the Early Jurassic Jordán Formation.

Major oxides composition														
Sample no.	**SiO_2**	**Al_2O_3**	**Fe_2O_3**	**CaO**	**MgO**	**Na_2O**	**K_2O**	**Cr_2O_3**	**TiO_2**	**MnO**	**P_2O_5**	**SrO**	**BaO**	**LOI**	**Total**
TGA-1	75.70	12.25	3.58	0.04	1.23	2.33	2.02	0.00	0.45	0.04	0.02	<0.01	0.04	3.72	101.42
TGA-3	68.90	13.80	5.33	0.07	1.40	1.22	2.53	0.01	1.01	0.11	0.03	<0.01	0.03	6.48	100.92

Trace and rare earth elements abundance															
Sample no.	**Pr**	**Rb**	**Sm**	**Sn**	**Sr**	**Ta**	**Tb**	**Th**	**Tm**	**U**	**V**	**W**	**Y**	**Yb**	**Zr**
TGA-1	17.65	67.10	14.25	2.50	70.70	1.10	1.64	10.00	0.58	1.83	45.00	3.60	49.40	4.13	191.00
TGA-3	9.02	85.30	7.13	2.20	38.30	1.20	1.10	8.15	0.65	2.43	124.00	1.70	37.10	3.74	370.00

Trace and rare earth elements abundance												
Sample no.	**Ag**	**As**	**Cd**	**Co**	**Cu**	**Li**	**Mo**	**Ni**	**Pb**	**Sc**	**Tl**	**Zn**
TGA-1	<0.50	<5.00	<0.50	9.00	3.00	20.00	2.00	24.00	11.00	8.00	<10.00	68.00
TGA-3	<0.50	<5.00	<0.50	16.00	4.00	30.00	1.00	23.00	19.00	13.00	<10.00	62.00

6.1. Significance of hydrothermal alteration

The analysis of mobile elements and their connection to alteration minerals was conducted using the alteration box of Large et al. (2001). Alteration effects are crucial to consider, as the volcaniclastic rocks are altered to varying extents based on petrographic observations and highly variable LOI values (from 3.72 to 6.48 wt.% for samples TGA-1 and TGA-3, respectively). Significant K-hydrothermal alteration is indicated when plotted outside the magmatic composition field in the igneous spectrum diagram of Hughes (1972), with sample TGA-1 closer to the igneous spectrum, indicating lesser alteration, and sample TGA-3 being more altered (Fig. 13a). The mobility of elements was assessed using the alteration box plot of Large et al. (2001). Fig. 13b confirms that the analyzed samples define a hydrothermal trend, transitioning from the least altered dacite box to intense pyritic alteration. Consequently, sample TGA-1 shows less alteration than sample TGA-3, suggesting that the major element compositions of TGA-1 are more reliable for geochemical examination. The presence of hydrothermal alteration highlights post-depositional processes that have influenced the geochemical composition of the rocks. The variation in alteration between these two samples also emphasizes the heterogeneity within the formation, which has implications for understanding the geological history of the region, including the interplay of volcanic activity, hydrothermal alteration, and subsequent diagenesis. Despite the effects of hydrothermal alteration, particularly in sample TGA-3, the consistency between petrographic features, mineralogical data, and whole-rock compositions allows for a meaningful interpretation of magmatic affinity and depositional processes.

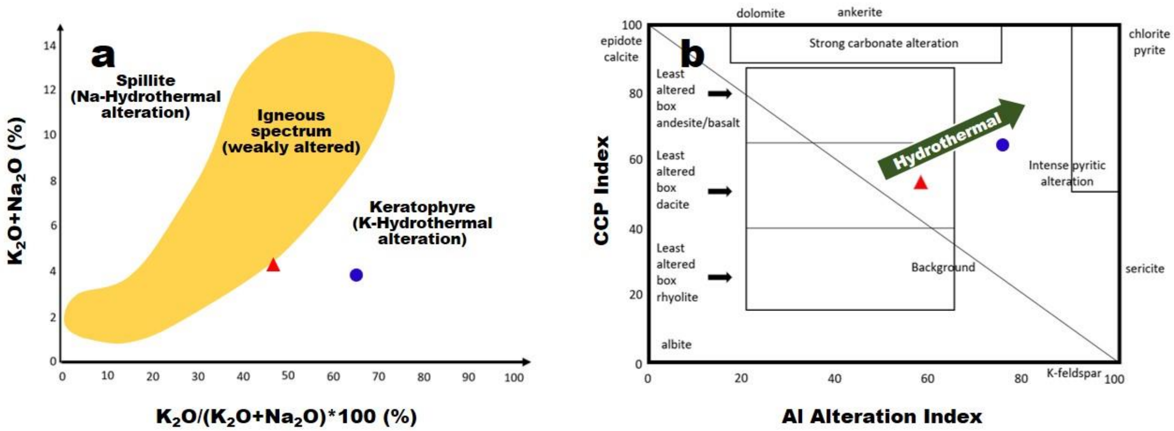

Fig. 13. (a) Igneous spectrum diagram of Hughes (1972) displaying the effects of alteration on the Jordan Formation´s volcaniclastic rocks. (b) Alteration box of Large et al. (2001), with compositions of various alteration minerals; rectangles represent least altered fields. TGA-1 and TGA-3 are indicated by a red triangle and a blue circle, respectively.

6.2. Classification and nomenclature

The geochemical composition of the analyzed tuffaceous rocks shows varying percentages of key elements: SiO_2 (75.7% and 68.9%), Al_2O_3 (12.25% and 13.80%), FeOt (3.58% and 5.33%), CaO (0.04% and 0.07%), MgO (1.23% and 1.40%), Na_2O (2.33% and 1.22%), K_2O (2.02% and 2.53%), and TiO_2 (0.45% and 1.01%). These elemental compositions align with the stability ranges for rhyolite, rhyodacite, and dacite. Various rock classification diagrams were employed for the classification and nomenclature of the Jordan Formation's volcaniclastic rocks. According to the Total Alkali vs. SiO_2 (TAS) diagrams by Middlemost (1994) and Le Bas et al. (1986), the samples fall within the rhyolite and near the dacite-rhyolite boundary (Figs. 14a-14b). However, the Zr/TiO_2 vs. Nb/Y diagram by Winchester and Floyd (1977) is more accurate as Zr and Ti are not mobile elements, and the samples fall in the rhyodacite/dacite field. Figs. 14c-14d show the Zr/TiO_2 vs. SiO_2 and Nb/Y vs. Zr/TiO_2

diagrams, where the samples fall in the rhyodacite/dacite and rhyolite fields. Additionally, the Al-Fe*+Ti-Mg triangular diagram by Jensen (1976) categorizes the rocks into the dacite field of the IV calc-alkaline series, at the boundaries of the tholeiitic and calc-alkaline series (Fig. 14e). The Ab-An-Or triangular diagram, showing normative plots for the Jordan Formation's volcaniclastic rocks, indicates that they correspond to a rhyolite according to O’Connor’s (1965) classification (Fig. 14f).

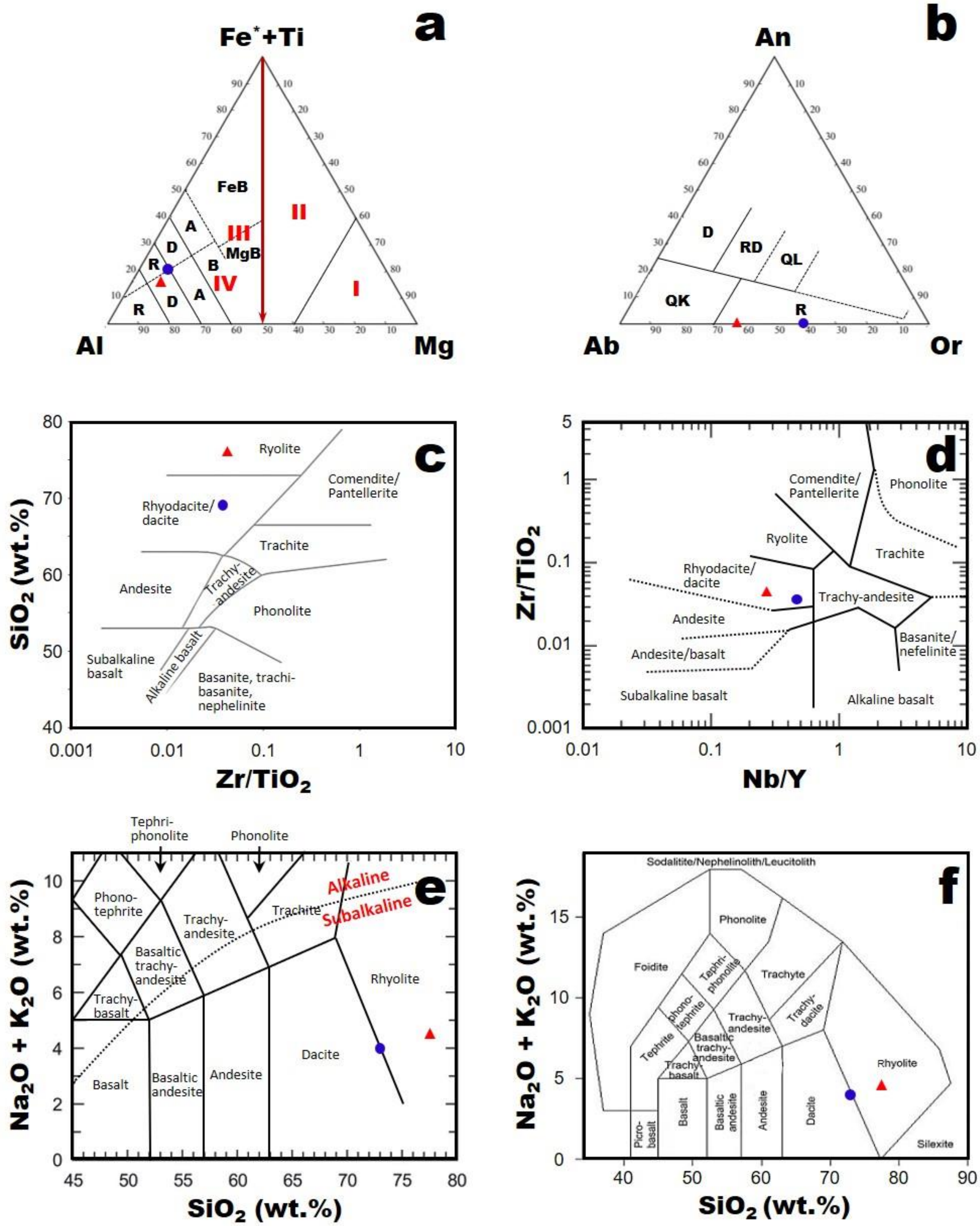

Fig. 14. Triangular diagrams of (a) Al-Fe*+Ti-Mg of Jensen (1976) and (b) Ab-An-Or of O'Connor (1965) for the Jordan Formation´s volcaniclastic rocks. (c) Zr/TiO_2 vs. SiO_2 and (d) Nb/Y vs. Zr/TiO_2 diagrams by Winchester and Floyd (1977) for the Jordan Formation´s volcaniclastic rocks. (e)-(f) TAS diagrams by Le Bas et al. (1986) and Middlemost (1994)

for the Jordan Formation´s volcaniclastic rocks. I, komatiites; II, komatiitic basalts; III, tholeiitic series (FeB: Fe-rich tholeiites, and MgB: Mg-rich tholeiites); IV, calc-alkaline series (B: basalt; A, andesite; D: dacite; R: rhyolite); QK, quartz keratophyre; R, rhyolite; D, dacite; RD, rhyodacite; QL, quartz latite.. TGA-1 and TGA-3 are indicated by a red triangle and a blue circle, respectively.

6.3. Magmatic series

In order to determination of magma series of the Jordan Formation´s volcaniclastic rocks different diagrams were used. According to the FeOt/MgO vs. SiO_2 diagram of Miyashiro (1974), which discriminates tholeiitic and calc-alkaline series, the analyzed volcaniclastic rocks fall in the field of calc-alkaline series (Fig. 15a). The K_2O vs. SiO_2 diagram of Peccerillo and Taylor (1976), which discriminates tholeiitic, calc-alkaline, high-K calc-alkaline and shoshonite series, and the rocks plot within the field of calc-alkaline series (Fig. 15b). The Na_2O+K_2O-FeOt-MgO (AFM) diagram proposed by Irvin and Baragar (1971) also discriminates tholeiitic and calc-alkaline series, and the rocks plot within the field of calc-alkaline series (Fig. 15c). These rocks plot in the field of calc-alkaline series in the Th/Yb vs. Zr/Y magmatic affinity diagram of Ross and Bedard (2009) as shown in Fig. 15d. The results from the classification diagrams, collectively establish a consistent characterization of the studied rocks as calc-alkaline in nature, as shown in Fig. 15. These geochemical features collectively support the interpretation of a calc-alkaline magmatic series, consistent with a volcanic arc setting. While the number of analyzed samples is limited, the convergence of petrographic, mineralogical, and geochemical indicators adds robustness to this interpretation.

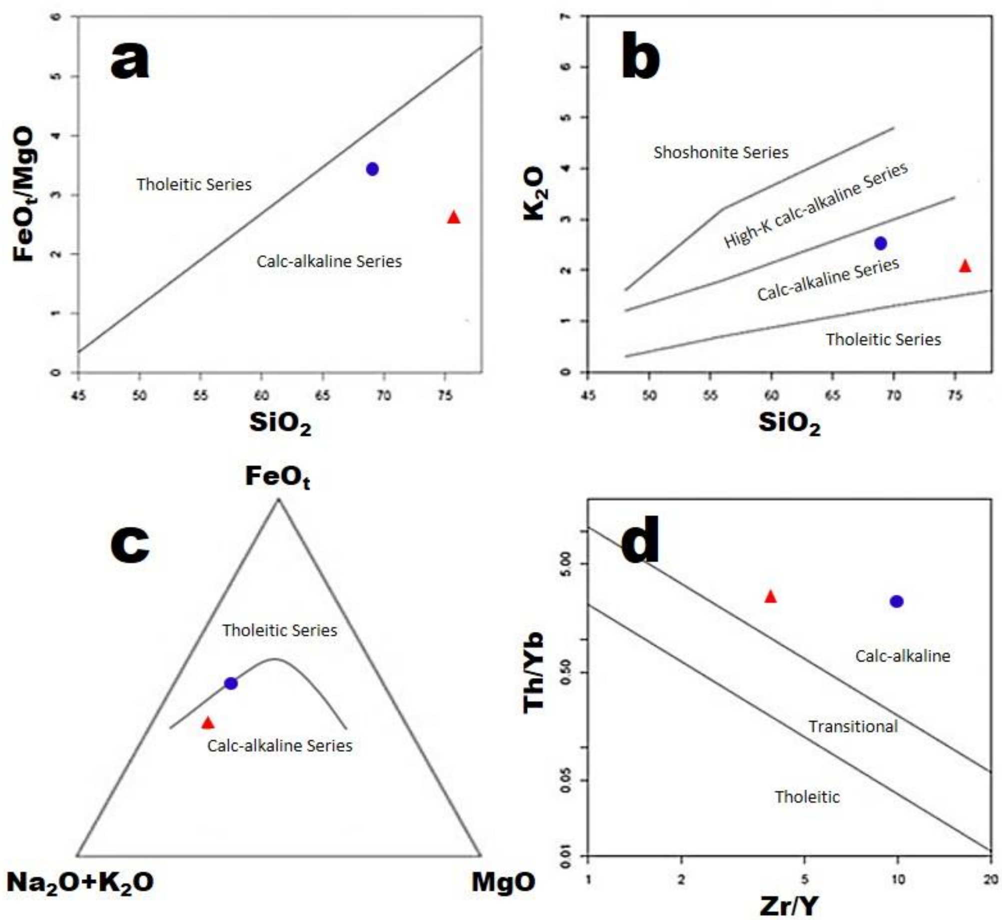

Fig. 15. Classification diagrams of (a) FeOt/MgO vs. SiO_2 of Miyashiro (1974), (b) K_2O vs. SiO_2 of Peccerillo and Taylor (1976), (c) Na_2O+K_2O-FeOt-MgO (AFM) of Irvine and Baragar (1971), and (d) Th/Yb vs. Zr/Y of Ross and Bedard (2009) for the Jordan Formation´s volcaniclastic rocks. TGA-1 and TGA-3 are indicated by a red triangle and a blue circle, respectively.

6.4. Tectonic discriminate diagrams

In order to define the tectonic setting of the Jordan Formation´s volcaniclastic rocks several tectonic discriminate diagrams have been used, which are described below. The geotectonic discrimination diagrams, as presented by Pearce et al. (1984), provide compelling evidence pointing toward a volcanic arc setting as the likely geotectonic environment for the tuffaceous rocks within the Jordan Formation, as depicted in Fig. 16a. On the other hand, the geotectonic discrimination diagrams proposed by Schandl and Gorton (2002), as shown in Fig. 16b, consistently indicate a Late Jurassic volcanic activity scenario, situated within the context of an active continental margin environment. Intriguingly, when we turn our attention to the diagram incorporating La/10-Y/15-Nb/8 ratios from Cabanis and Lecolle (1989) and illustrated in Fig. 17a, we uncover an additional layer of insight. This specific diagram suggests that these rocks were formed within an active compressive orogenic setting. Fig. 17b shows a Th/Yb vs. Ta/Yb diagram of Bowden et al. (1984), which reveals a compelling alignment between the analyzed samples and the characteristic calc-alkaline nature of rocks commonly encountered in the Central Andes.

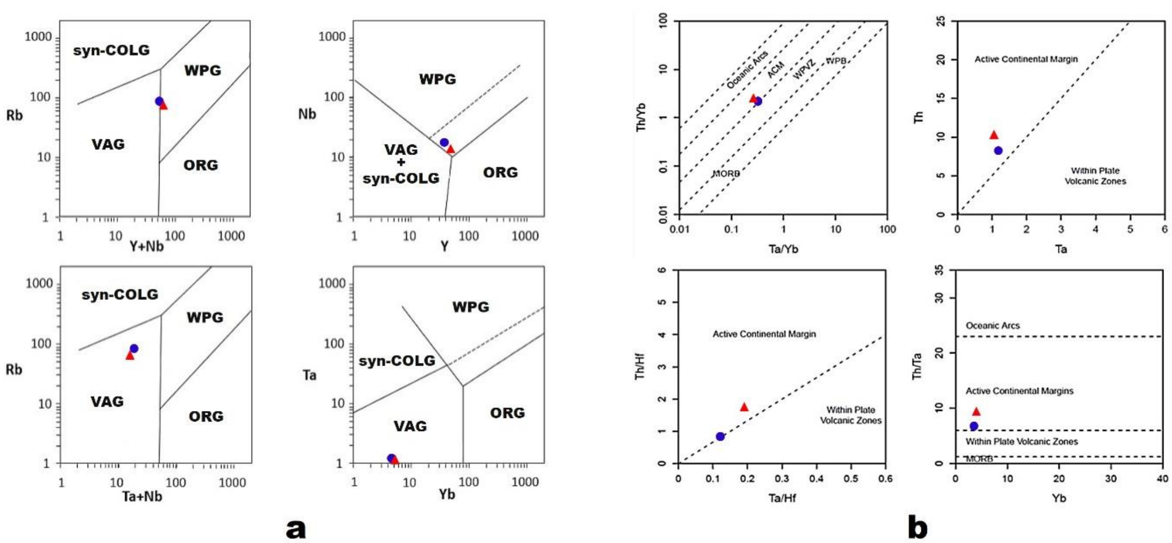

Fig. 16. Tectonic discrimination diagrams for the Jordan Formation´s volcaniclastic rocks after (a) Pearce et al. (1984) for Rb vs. Y+Nb, Nb vs. Y, Rb vs. Ta+Nb, and Ta vs. Yb, and (b) Schandl and Gorton (2002) for Ta/Yb vs. Th/Nb, Ta vs. Th, Ta/Hf vs. Th/Hf, and Yb vs Th/Ta. ORG, ocean-ridge granite; syn-COLG, syn-collisional granite; VAG, volcanic arc

granite; WPG, within-plate granite. TGA-1 and TGA-3 are indicated by a red triangle and a blue circle, respectively.

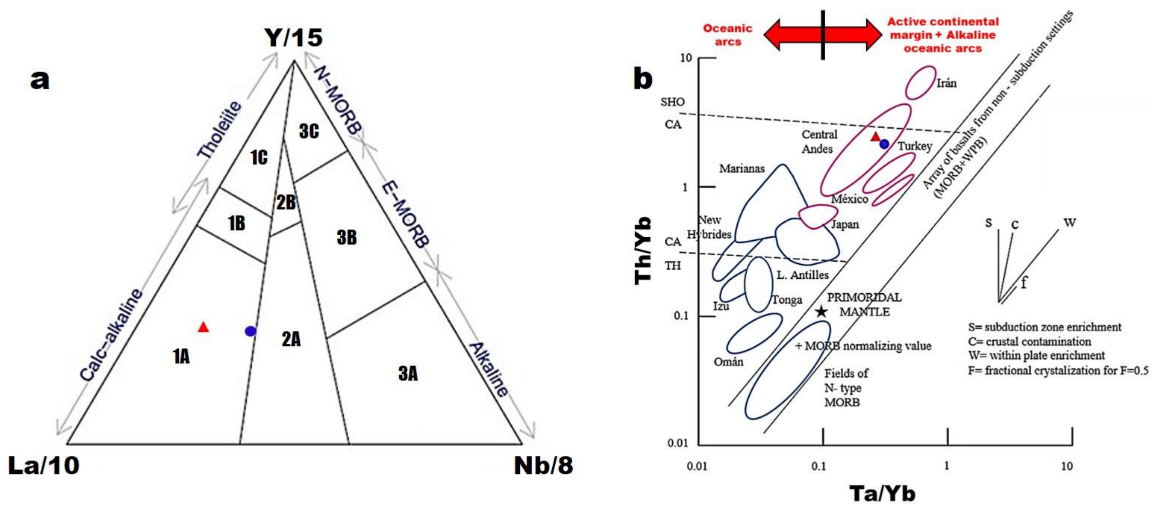

Fig. 17. (a) La/10-Y/15-Nb/8 tectonic discrimination diagram of Cabanis and Lecolle (1989) for the Jordan Formation´s volcaniclastic rocks. (1) Orogenic domain (volcanic arc basalts): 1A, calc-alkaline basalts; 1B, overlap between 1A and 1C; 1C, volcanic arc tholeiites. (2) Late- to post-orogenic intra-continental domain (continental basalts): 2A, continental basalts; 2B, back-arc basalts. (3) Anorogenic domain (oceanic basalts): 3A, alkaline basalts; 3B, EMORB; 3C, N-MORB. (b) Th/Yb vs. Ta/Yb tectonic discrimination diagram of Bowden et al. (1984) of the Jordan Formation´s volcaniclastic rocks. TGA-1 and TGA-3 are indicated by a red triangle and a blue circle, respectively.

6.5. Chondrite-normalized REE patterns and multi-element "spider" diagrams

Fig. 18 shows the chondrite-normalized REE patterns and multi-element "spider diagrams" for the Jordan Formation´s volcaniclastic rocks. According to the chondrite-normalized REE patterns (Fig. 18a), the analyzed samples reveal a similar trend, having fairly steep abundances of light rare earth elements (LREE), and relatively flat abundances of heavy rare earth elements (HREE). The LREE patterns also show negative Eu anomalies, characteristic of calk-alkaline magmas. However, sample TGA-1 also shows a negative Ce anomaly. Fig. 18b shows the spider diagrams of trace elements normalized to the primitive mantle of Sun and McDonough (1989), which reveal a high similarity with negative anomalies of Ba, Nb, P, and Ti, and a positive anomaly of Pb, which are geochemical characteristics correlating with subduction tectonic environments.

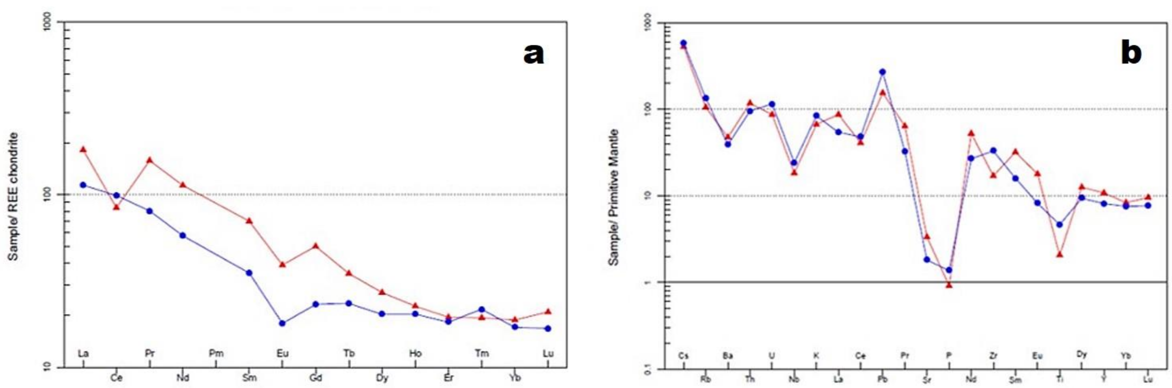

Fig. 18. (a) Chondrite-normalized REE patterns (Nakamura, 1974), and (b) Primitive mantle-normalized spider diagram for trace elements (normalized data from Sun and McDonough, 1989) for the Jordan Formation´s volcaniclastic rocks. TGA-1 and TGA-3 are indicated by red triangles and blue circles, respectively.

7. Discussion

7.1. Provenance

7.1.1. Evidence from petrography

The petrographic analysis of the volcaniclastic rocks from the Jordan Formation offers insights into their potential provenance. The presence of lithic fragments primarily composed of felsic volcanic rocks, notably rhyolitic tuffs, suggests that these rocks may have originated from volcanic sources within the region. The inclusion of juvenile crystal fragments, such as K-feldspar, plagioclase, and quartz, along with occasional muscovite and biotite, is consistent with the mineral assemblage commonly found in volcanic rocks. The presence of metamorphic lithic fragments resembling the lithologies of the San Pedro's Phyllites further supports a local origin for these rocks. These observations collectively indicate a proximal source for the Jordan Formation's volcaniclastic rocks, pointing to nearby volcanic activity within the tectonic framework of the region.

7.1.2. Evidence from geochemistry

Geochemical data provides a valuable window to explore the provenance of the rocks analyzed in this study. A significant indicator arises from the variability in LOI values observed in the analyzed samples, which reflects different degrees of alteration in these rocks. It is particularly noteworthy that TGA-1 appears significantly fresher compared to TGA-3, which exhibits distinct signs of potassic hydrothermal alteration, as confirmed in the diagrams by Hughes (1972) and Large et al. (2001) in Fig. 13. These findings not only corroborate the interpretation of the geochemical data but also align with previous macroscopic and microscopic analyses conducted on the samples. The presence of hydrothermal alteration raises intriguing questions about the post-depositional processes that have influenced the geochemical composition of these rocks. Furthermore, the variability in the degrees of alteration between these two samples underscores the inherent heterogeneity within the studied formation. This heterogeneity in the rock characteristics within the same formation suggests multiple possible sources for these materials. To precisely understand the provenance of these rocks, it is essential to carry out further research, including more detailed geochemical analysis and a broader consideration of the geological conditions and processes that have shaped this formation.

7.2. Tectonic setting

The petrographic characteristics of the volcaniclastic rocks from the Jordan Formation provide clues about the tectonic setting in which these rocks were deposited. The presence of crystal-rich tuffs with variable grain size dispersion suggests a dynamic and high-energy depositional environment, possibly associated with volcanic eruptions. Additionally, the occurrence of flame structures and eutaxitic textures characteristic of ignimbrites points to pyroclastic activity, which could be linked to subduction-related volcanic events. The presence of oxide patinas covering the vitreous matrix may indicate alteration under specific environmental conditions. Furthermore, the lack of clear associations between pyroclasts and the matrix initially raises questions about their origin. However, when considered in conjunction with field observations, a consolidated volcaniclastic deposition origin within a tectonic framework associated with volcanic activity seems the most plausible explanation.

The volcaniclastic rocks of the Jordan Formation show evidence of hydrothermal alteration, suggesting that they underwent geological processes subsequent to their initial deposition. This becomes evident when observing the variability in LOI values and differences in the degrees of alteration between samples TGA-1 and TGA-3, as shown in Fig. 13. These alteration processes likely had a significant impact on the chemical composition of the rocks. These secondary processes are important in understanding the post-depositional alterations that have influenced the composition of the rocks. The recognition of these secondary processes adds depth to our interpretation. It suggests that the geochemical signatures of the rocks are not static but can undergo modifications over geological time scales. This, in turn, prompts further inquiries into the timing, mechanisms, and implications of these secondary alterations, contributing to a more nuanced understanding of the geological history and evolution of the Jordan Formation´s volcaniclastic rocks. The robust alignment across multiple classification systems underscores the reliability of this assessment and emphasizes the dominant geochemical profile of the samples. Moreover, it is worth noting the subtle chemical variations observed within the samples, particularly towards peraluminosity and peralkalinity. These variations may be indicative of secondary processes, specifically the alteration of tuffaceous fragments composed of alkali feldspar and quartz through the devitrification process, as well as the palagonitization of volcanic glass. The chemical composition of the rocks, as illustrated in Fig. 14 indicates that the samples fall within the fields of rhyodacite/dacite and rhyolite in various classification diagrams. These fields are characteristic of volcanic rocks with intermediate to acidic compositions, which are typical of felsic volcanic activity and subduction tectonic processes in the context of a volcanic arc. The abundance of SiO_2 (75.7-68.9%), indicates that these rocks have a felsic nature. This suggests they have undergone a geological history influenced by volcanic processes, such as magmatic activity and magma evolution. Furthermore, the low levels of CaO (0.04-0.07%), MgO (1.23-1.40%), and FeOt (3.58-5.33%) imply a limited contribution from mafic minerals. These results are consistent with a predominantly felsic nature of the rocks. The minor elements in the composition of these rocks also provide valuable insights. The levels of Na_2O (2.33-1.22%) and K_2O (2.02-2.53%) indicate a potential enrichment in alkali feldspar minerals. This could be related to tectonic processes, such as plate subduction or igneous activity in a volcanic arc setting. These observations offer valuable insights into the petrogenesis of the rocks and provide initial indications of their tectonic setting. Although most geochemical diagrams (Figs. 15–17) suggest a calc-alkaline affinity typical of subduction-related magmatism, the presence of rhyolitic tuffs and the inferred volcanic processes within a fluvio-lacustrine setting also support the possibility of localized extensional tectonics, potentially associated with back-arc or intra-arc rifting. This interpretation does not necessarily exclude a subduction setting; rather, it points to the coexistence of transtensional tectonics within an overall convergent margin scenario, as proposed by Zuluaga and López (2019), where oblique convergence leads to local extension and basin development. To gain a comprehensive understanding of these aspects, further geochemical analysis and interpretation utilizing these diagrams are warranted. This approach promises to unravel the intricate geological history and processes that have shaped the analyzed volcaniclastic rocks, ultimately enhancing our comprehension of the broader geological context in which they are situated. The magmatic affinity diagrams (Fig. 15) suggest that the rocks belong to the calc-alkaline series, hinting at a geological environment related to magmatic activity in the context of an active continental margin. This magmatic series is characterized by a chemical element ratio consistent with processes of melting in a specific geotectonic setting. Figs. 16a-16b and 17a-17b provide valuable clues about the geological environment in which these rocks likely originated. They indicate that the Jordan Formation´s volcaniclastic rocks formed in a volcanic environment probably in the context of an active continental margin with magmatic activity. Furthermore, Fig. 17a suggests the potential influence of compressional orogenic processes in the evolution of these rocks. The anomalies in the rare and trace element patterns (Fig. 18) indicate that the rocks of the Jordan Formation underwent specific geological processes that left their mark on their chemical composition. The chondrite-normalized REE patterns (Fig. 18a) of the analyzed samples reveal a similar trend, having fairly steep abundances of light rare earth elements (LREE), and relatively flat abundances of heavy rare earth elements (HREE). Based on the similarity and subhorizontal trend of the HREE pattern, it is proposed that both samples have similar sources and share similar geochemical characteristics in relation to heavy rare earth elements. This can have several implications for the origin of the samples. However, in this study, it is suggested that the two samples have a common origin, meaning they may have been formed from the same magmatic source or are geologically related in terms of their evolutionary history. This could indicate that they come from the same geographic area or experienced similar geological processes in the past. Nonetheless, a precise interpretation of the origin based on the HREE pattern would require a more detailed analysis considering other geochemical elements, mineralogy, and the general geological context of the samples. On the other hand, the negative Eu and Ce anomalies in LREE patterns are typical of calk-alkaline magmas formed in geotectonic environments (subduction zones) where the lithospheric plate undergoes processes of melting and fractionation. These elements were retained by the source feldspar during partial melting or were removed by fractional crystallization of the plagioclase. Spider diagrams normalized to the primitive mantle (Fig. 18b) reveal (1) negative anomalies in Ba, Nb, P, and Ti, which suggests a relative deficiency of these elements compared to the reference primitive mantle associated to subduction tectonic environments, and (2) a notable positive anomaly in Pb, which indicates a higher concentration of this element in the analyzed rocks compared to the primitive mantle, possibly related to subduction processes through the mobilization of this element during interaction with hydrothermal fluids. These geochemical patterns probably do not provide a definitive answer regarding the exact geological environment in which the Jordan Formation´s volcaniclastic rocks formed. However, they suggest that these rocks experienced geotectonic processes consistent with the previous interpretation of a volcanic environment, possibly an active continental margin, and potentially influenced by orogenic processes. The post-depositional hydrothermal alteration processes are indicative of the subsequent geological evolution of these rocks.

The petrology study of the Lower Jurassic Jordan Formation's volcaniclastic rocks at the Mesa de San Pedro provides several points of international importance for researchers and geologists. These are presented below. The recognition of hydrothermal alteration, which has broader implications for understanding the geological history and post-depositional processes in volcaniclastic rocks worldwide. The alignment between the analyzed samples and the characteristic calc-alkaline nature of rocks commonly encountered in the Central Andes is a valuable observation. The use of geotectonic discrimination diagrams allows for a refined interpretation of the tectonic setting of the Jordan Formation at the Mesa de San Pedro. In particular, the geochemical evidence suggests a possible transition between volcanic arc-related magmatism and compressive orogenic processes. This observation, which has not been previously reported in this area, provides new data to assess the complex tectonomagmatic evolution of the northern Andes during the Lower Jurassic, a topic of growing interest in regional and global geological frameworks. The recognizing of secondary processes such as devitrification and palagonitization adds depth to the interpretation and prompts further inquiries into the timing, mechanisms, and implications of these alterations, providing an improved understanding on the evolution of volcaniclastic rocks. The major and trace element composition of the analyzed samples offers valuable insights into the petrogenesis of the rocks and provides initial indications of their tectonic setting. The chondrite-normalized REE patterns reveal enrichment in LREE and specific anomalies, such as Ce and Eu, which may be associated with sedimentary material contribution, fluid interaction, hydrothermal alteration, and plagioclase fractionation, adding to the understanding of the petrogenesis and post-depositional history of the rocks and contributing to the broader knowledge of geological processes that can apply to similar formations worldwide. Trace element anomalies indicate a subduction-related tectonic setting, providing insights into the geodynamic evolution of the region and offering implications for understanding similar tectonic environments in analogous geological contexts worldwide.

7.3. Tectonic and magmatic processes

A combination of U/Pb geochronology, ignimbrite, and tuff data within the Jordan Formation hints at concurrent tectonic and magmatic processes. According to Alarcón et al. (2020), it is likely that the volcanic edifices were emplaced on the metamorphic basement of the Santander Massif, as evidenced by the presence of accidental metamorphic lithics in the ignimbrites and tuffs. These findings support the notion that, during the fluvio-lacustrine sedimentation phase in which the Jordan Formation´s red beds were deposited, lava flows were simultaneously emplaced. Zuluaga and López (2019) proposed that the elongated configuration of plutons within the Santander Massif exerted control over the genesis and emplacement of magmatic pulses, possibly due to a transtensive crustal dynamic associated with oblique convergence in the subduction zone. They also suggested that the concurrent extension during magmatic activity could have contributed to the formation of basins during the emplacement of the Santander Plutonic Group. The ages obtained for the tuffs in the Jordan Formation, closely resembling those of the Santander Plutonic Group´s intrusives, indicate that volcanic activity likely occurred in the same magmatic event and concurrently with the fluvial-lacustrine sedimentation of the Jordan Formation. This supports a dynamic tectonic regime, in which subduction-related magmatism coexisted with localized extensional tectonics, facilitating magma ascent and explosive volcanic activity.

7.4. Synchronous sedimentation

The volcanosedimentary sequence of interest of the Jordan Formation can be classified as a muddy-sandy and tuffaceous facies. These layers are characterized by interbedded mudstones and very fine-grained sandstones, as well as thin layers of volcaniclastic rocks (tuffs and muddy tuffs). The presence of mudstone-sandstone layers suggests sedimentation through the settling of suspended materials under environmental conditions of low energy and discharge, with intermittent interruptions by ash falls, reflecting shallow and distal fluvial-lacustrine deposits. The limited horizontal distribution and substantial thickness of the ignimbrite bodies within the Jordan Formation imply that pyroclastic density currents, generated during volcanic activity, were significantly influenced by paleotopography (Walker, 1983), restricting the lateral spread of these volcanic products. The volcaniclastic rocks exposed in the Jordan Formation at the Mesa de San Pedro are believed to have formed through a series of small to moderately-sized eruptions from a monogenetic volcanic source. It is inferred that these volcaniclastic rocks represent sporadic and scattered volcanism that interacted with a fluvio-lacustrine sedimentary environment. We propose the existence of a rift zone in this context, which likely facilitated the formation of rhyolitic tuffs through the ascent of migrating magma and interactions with surface water. This rift-like tectonic activity may reflect local extensional structures superimposed on a broader subduction context, compatible with back-arc extension or transtensional tectonics in a convergent setting. Therefore, the Jordan Formation sequence represents episodic volcaniclastic deposition under fluvial-lacustrine conditions and likely corresponds to distal facies. Explosive volcanism can introduce substantial volumes of primary pyroclastic clasts into various sedimentary settings, both terrestrial and/or marine, where they can be remobilized, reworked, and redeposited (e.g., Palmer and Shawkey, 2001; Manville et al., 2009). The presence of opaque minerals, as suggested by Abdel-Motelib et al. (2015), indicates multiphase reworking and prolonged oxidation of the limited vegetation cover, indicative of an oxidizing environmental condition. This, in turn, provides valuable insights into the prevailing environmental conditions, particularly suggesting a protracted period of oxidation and an environment characterized by high levels of oxygen. Such findings could have significant implications for our understanding of past ecological dynamics and the interplay between geological and environmental factors over time. The presence of these opaque minerals not only serves as a record of geological transformation but also offers a window into the dynamic relationship between geology and ecology. This interplay is a critical aspect of understanding the environmental history of a region, as prolonged oxidation can influence the evolution of plant communities and their adaptations. The revelation of multiphase reworking suggests a complex geological history that may have been influenced by various external factors, further emphasizing the need for interdisciplinary research to comprehend the full extent of these processes.

7.5. Tectonic synthesis and implications

The apparent contradiction between geochemical evidence suggesting subduction-related magmatism and sedimentological indications of rift-related volcanism can be reconciled through a more nuanced interpretation of the tectonic evolution of the region, particularly in the context of the Jordan Formation. The geochemical signatures within the Jordan Formation, including calc-alkaline affinities, negative Eu and Ce anomalies, and trace element patterns consistent with subduction zones, suggest that the magmas originated in a volcanic arc setting, typical of active continental margins. However, sedimentary and volcanosedimentary characteristics, such as fluvio-lacustrine deposits, tuffaceous facies, and pyroclastic flows confined by paleotopography, indicate the presence of localized extensional regimes (Alarcón et al., 2020; Zuluaga and López, 2019). This duality may reflect a tectonic scenario of transtensional dynamics within an overall convergent margin, where oblique subduction created localized extensional zones that facilitated volcanic activity and basin formation. This type of mixed tectonic regime is not exclusive to the Northern Andes, but has also been documented in other tectonically active regions worldwide. In the Gulf of California, Lizarralde et al. (2007) observed a variety of rifting styles, where narrow rifts with robust magmatism contrast with wide rifts that are relatively magma-poor. This variability is linked to mantle depletion and suggests that fertile mantle regions, potentially influenced by sedimentary insulation, promote intense volcanic activity in certain rift segments. Schmitt et al. (2013) further explored the geochemistry of volcanic rocks in the northern Gulf of California, confirming that both oceanic rifting and subduction-related processes contribute to the region's complex geological evolution. In the South China Sea, Chao (2021) explored the transition from continental rifting to early seafloor spreading at the tip of the NW South China Sea propagator, where both extensional and compressional dynamics occur. In this case, subduction-driven magmatism coexists with rift-related volcanism, particularly in areas affected by oblique subduction and localized extension. Furthermore, Michaud et al. (2006) described a similar tectonic setting along the Baja California margin, where the subduction of the Farallon plate and the rotation of spreading centers induced transtensional deformation, generating magmatic systems linked to both subduction and rifting processes. The geodynamic processes of the Domeyko Basin in northern Chile provide another relevant example of transtensional tectonics in a subduction-related rift basin, where synrift volcanism and sedimentation are influenced by both extension and subduction dynamics (Espinoza et al., 2019). Additionally, the East African Rift System displays similar mixed tectonic environments, where rifting and magmatism influenced by both extension and oblique subduction interact to produce complex geological features

(Ziegler and Cloetingh, 2004). This tectonic synthesis provides a coherent explanation that integrates petrographic, geochemical, and stratigraphic data, offering a robust framework for understanding the complex evolution of the Jordan Formation and its broader regional tectonic context. By comparing the Northern Andes with other globally recognized tectonic settings, we gain a deeper insight into the interplay of subduction, rifting, and magmatic processes that define their geodynamic evolution.

8. Conclusions

In this geological study, significant findings have contributed to a better understanding of the geological features in the northwestern region of South America. The first-time identification of volcaniclastic rocks (tuffs) within the Lower Jurassic Jordan Formation in the Mesa de San Pedro, Colombia, has implications that extend beyond the local context, significantly enriching the wider body of knowledge in the field of Earth sciences. The primary conclusions of this research are as follows:

- Important lithological contacts and stratigraphic relationships have been identified in the Mesa de San Pedro, placing the Jordan Formation within a sequence of Early Jurassic age. This identification challenges previous interpretations and makes a valuable contribution to the geological understanding of the region.
- Petrographic and geochemical analysis suggests a nearby source for these rocks, possibly related to volcanic activity in the region, which is supported by the presence of felsic and metamorphic lithologic fragments, and indicates a high-energy environment, possibly associated with volcanic eruptions and subduction-related activity.

- Hydrothermal alteration following deposition is reflected in sample variability, highlighting formation heterogeneity and implying multiple potential sources.
- Geochronological data suggests that volcanic activity occurred concurrently with fluvial-lacustrine sedimentation. This volcanic activity appears to be related to the uplift of volcanic edifices on the metamorphic basement.
- The Jordan Formation sequence represents synchronous deposition of volcanic tephra in a fluvial-lacustrine environment. The limited horizontal distribution and thickness of the ignimbrites suggest that pyroclastic flows were influenced by paleotopography. The presence of opaque minerals indicates a long period of oxidation and high oxygen conditions.
- This study provides a valuable contribution to the understanding of the geology of the Santander Massif and its geological context in northern South America. The results underscore the significance of the Jordan Formation in the region and emphasize the need for future research to expand our knowledge of the geological evolution of this area.

Acknowledgements

We would like to express our gratitude to the Universidad de Pamplona and Universidad Industrial de Santander, which provided fieldwork and analytical facilities in advancing our understanding of the Jordan Formation and its relationship with volcanic activity in the Mesa de San Pedro region. We also want to thank these institutions that provided financial and logistical support to carry out this research. The authors would also like to acknowledge the anonymous referees for their critical and insightful reading of the manuscript and are most grateful to the above-named people and institutions for support. Furthermore, we would like to acknowledge the local community and the individuals who provided their collaboration during the fieldwork. Their knowledge and hospitality were immensely valuable in conducting this study in the area. Lastly, we want to recognize the teamwork and dedication of our own research team. Each member brought their expertise and skills, which were instrumental in the success of this study.

References

Abdel-Motelib, A.; Kabesh, M.; El Manawi, A.H.; Said, A. 2015. Oligocene lacustrine tuff facies, Abu Treifeya, Cairo-Suez Road, Egypt. J. Afr. Earth Sci. 102: 33–40.

Alarcón, C.M.; Rodríguez, J.G. 2019. Stratigraphy, facies, and sedimentation paleoenvironment of the Jordan Formation, a fluvio-lacustrine record with volcanic activity incidence. Undergraduate Thesis, Industrial University of Santander: 130 p.

Alarcón, C.M.; Clavijo, J.; Mantilla, L.C.; Rodríguez, J.G. 2020. New age proposal for the sedimentary record of the Bocas and Jordan formations and their relationship with the development of magmatic activity of the Santander Plutonic Group, Eastern Cordillera, Colombia. Rev. Acad. Colomb. Cienc. Ex. Fís. Nat. 44 (173): 1137-1151.

Ayala-Calvo, R.; Veloza-Fajardo, G.; Bayona, G.; Gómez-Casallas, M.; Rapalini, A.; Costanzo-Álvarez, V.; Aldan, M.; Cortes, M. 2005. Paleomagnetism and Magnetic Mineralogy in the Mesozoic Units of Bucaramanga and the Floresta Massif. Geol. Colombiana 30: 49-66.

Bayona, G.; Jiménez, G.; Silva, C.; Cardona, A.; Montes, C.; Roncancio, J.; Cordani, U. 2010. Paleomagnetic data and K–Ar ages from Mesozoic units of the Santa Marta Massif, A preliminary interpretation for block rotation and translations. J. South Am. Earth Sci. 29 (4): 817-831.

Bayona, G.; Bustamante, C.; Nova, G.; Salazar–Franco, A.M. 2020. Jurassic evolution of the northwestern corner of Gondwana: Present knowledge and future challenges in studying Colombian Jurassic rocks. In: Gómez, J.; Pinilla–Pachón, A.O. (Eds), The Geology of Colombia, Volume 2: Mesozoic. Publ. Geol. Especiales SGC 36, Bogotá: 161–202.

Belica, M.E.; Tohver, E.; Pisarevsky, S.A.; Jourdan, F.; Denyszyn, S.; George, A.D. 2017. Middle Permian paleomagnetism of the Sydney Basin, eastern Gondwana: Testing Pangaea models and the timing of the end of the Kiaman Reverse Superchron. Tectonophysics 699: 178–198. https://doi.org/10.1016/j.tecto.2017.01.018

Bowden, P.; Batchelor, R.A.; Chappell, B.W.; Didier, J.; Lameyre, J. 1984. Petrological, geochemical and source criteria for the classification of granitic rocks: a discussion. Phys. Earth Planet. Interiors 35 (1–3): 1-11.

Cabanis, B.; Lecolle, M. 1989. The La/10-Y/15-Nb/8 diagram: a tool for discriminating volcanic series and highlighting processes of mixing and/or crustal contamination. Compt. Rend. Acad. Sci. Ser. 2 - Mécanique, Phys. Chim. Sci. Univ. Terre 309: 2023–2029.

Castellanos, O.M.; Ríos, C.A. 2008. Geological Itinerary of the Crystalline Basement in the Southwestern Region of the Santander Massif. Editorial Java - ISBN 978-958-98060-9-8, 93p.

Cediel, F. 1968. The Girón Group: A Mesozoic Molasse of the Eastern Cordillera. Bol. Geol. 16 (1-3): 5-96.

Cediel, F.; Shaw, R.P.; Cáceres, C. 2003. Tectonic assembly of the northern Andean Block. In: Bartolini, C.; Buffler, R.T.; Blickwede, J. (Eds), The Circum–Gulf of Mexico and the Caribbean: Hydrocarbon habitats, basin formation, and plate tectonics. Am. Assoc. Petrol. Geol. Mem. 79, Tulsa: 815–848.

Chao, P. 2021. Tectono-sedimentary and magmatic evolution of rifting and early seafloor spreading in the NW propagator to the South China Sea. PhD Thesis, Université de Strasbourg: 258 p.

Clavijo, J.; Mantilla, L.; Pinto, J.; Bernal, L.; Pérez, A. 2008. Geological Evolution of the San Lucas Range, Northern Middle Magdalena Valley, and Northwest of the Eastern Cordillera. Boletín Geol. 30 (1): 45-62.

Cohen, K.M.; Finney, S.C.; Gibbard, P.L.; Fan, J.X. 2020. The ICS International Chronostratigraphic Chart. Episodes 36: 199-204. https://doi.org/10.18814/epiiugs/2020/019027

Cochrane, R.; Spikings, R.; Gerdes, A.; Ulianov, A.; Mora, A.; Villagómez, D.; Putlitz, B.; Chiaradia, M. 2014. Permo–Triassic anatexis, continental rifting and the disassembly of western Pangaea. Lithos 190–191: 383–402.

Colmenares, L.; Zoback, M.D. 2003. Stress field and seismotectonics of northern South America. Geology 31 (8): 721-724.

Espinoza, M.; Montecino Jara, D.; Oliveros, V.; Astudillo, N.I.; Vásquez, P.; Reyes, R.; Celis, C.; González, R.; Contreras, J.F. 2019. The synrift phase of the early Domeyko Basin (Triassic, northern Chile): Sedimentary, volcanic and tectonic interplay in the evolution of an ancient subduction-related rift basin. Basin Res. 31(1): 4-32. https://doi.org/10.1111/bre.12305

Franzese, J.R.; Spalletti, L.A. 2001. Late Triassic - Early Jurassic continental extension in South Western Gondwana: Tectonic segmentation and pre-break-up rifting. J. South Am. Earth Sci. 14: 257-270.

Goldsmith, R.; Marvin, R.F.; Mehnert, H.H. 1971. Radiometric ages in the Santander Massif, Eastern Cordillera, Colombian Andes. U.S. Geol. Surv. Prof. Pap. 750: 44-49.

Horton, B.K.; Anderson, V.J.; Caballero, V.; Saylor, J.E.; Nie, J.; Parra, M.; Mora, A. 2015. Application of detrital zircon U-Pb geochronology to surface and subsurface correlations of provenance, paleodrainage, and tectonics of the Middle Magdalena Valley Basin of Colombia. Geosphere 11 (6): 1790-1811.

Hughes, C.J. 1972. Spilites, keratophyres, and the igneous spectrum. Geol. Mag. 109: 513–527.

Irvine, T.N.; Baragar, W.R.A. 1971. A guide to the chemical classification of the common volcanic rocks. Can. J. Earth Sci. 8: 523–548.

Janoušek, V.; Farrow, C.M.; Erban, V. 2006. Interpretation of whole-rock geochemical data in igneous geochemistry: introducing Geochemical Data Toolkit (GCDkit). J. Petrol. 47: 1255–1259.

Jaramillo, L.; Ward, D.E.; Téllez, N.A.; Cruz, J.A. 1969. Geology of part of quadrangles I-12 San Gil I-13 Málaga, Colombia Zone III. Natl. Inst. Geol. Min. Res. (INGEOMINAS), 70 p.

Jensen, L.S. 1976. A New Cation Plot for Classifying Subalkalic Volcanic Rocks. Ont. Geol. Surv. Misc. Pap. 66. Ministry of Natural Resources, 22 p. Toronto.

Jiménez, G.; García, H.; Geissman, J.W. 2021. Magnetostratigraphy and magnetic properties of the Jurassic to Lower Cretaceous Girón Group (northern Andes, Colombia). Geosphere 17 (6): 2172–2196.

Large, R.R.; Gemmell, J.B.; Paulick, H.; Huston, D.L. 2001. The Alteration Box Plot: A Simple Approach to Understanding the Relationship between Alteration Mineralogy and Lithogeochemistry Associated with Volcanic-Hosted Massive Sulfide Deposits. Econ. Geol. 96 (5): 957–971.

Le Bas, M.J.; Le Maitre, R.W.; Streckeisen, A.; Zanettin, B. 1986. A chemical classification of volcanic rocks based on the total alkali–silica diagram. J. Petrol. 27: 745–750.

Leal-Mejía, H. 2011. Phanerozoic Gold Metallogeny in the Colombian Andes: A tectono-magmatic approach. Doctoral Thesis, Universitat de Barcelona: 989 p.

Lizarralde, D.; Axen, G.; Brown, H.E.; Fletcher, J.; Gonzalez-Fernandez, A.; Harding, A.J.; Holbrook, S.; Kent, G.; Paramo, P.; Sutherland, F.; Umhoefer, P. 2007. Variation in styles of rifting in the Gulf of California. Nature 448(7152): 466-469. https://doi.org/10.1038/nature06035

Mantilla, L.C.; Bissig, T.; Cottle, J.M.; Hart, C.J.R. 2012. Remains of early Ordovician mantle-derived magmatism in the Santander Massif (Colombian Eastern Cordillera). J. South Am. Earth Sci. 38: 1-12.

Mantilla, L.C.; García, C.A.; Valencia, V.A. 2016. Proposal for the division of the so-called “Silgará Formation”, Santander Massif, Colombia, based on U-Pb ages in detrital zircons. Boletín Geol. 38 (1): 33-50.

Manville, V.; Segschneider, B.; Newton, E.; White, J.D.L.; Wilson, C.J.N.; Houghton, B.F. 2009. Environmental impact of the 1.8 ka Taupo eruption: Landscape responses to a large-scale explosive rhyolite eruption. In: Nemeth, K.; Manville, V.; Kano, K. (Eds), Source to Sink: From volcanic eruptions to volcaniclastic deposits on the Pacific Rim. Sediment. Geol. 220: 318–336.

Mann, P.; Escalona, A.; Castillo, M.V. 2006. Regional geologic and tectonic setting of the Maracaibo supergiant Basin, western Venezuela. Am. Assoc. Petrol. Geol. Bull. 90 (4): 445–477.

Maze, W. 1984. Jurassic La Quinta Formation in the Sierra de Perijá, northwestern Venezuela: Geology and tectonic environment of red beds and volcanic rocks. In: Bonini, W.; Hargraves, R.; Shagam, R. (Eds), The Caribbean–South American Plate Boundary and Regional Tectonics. Geological Society of America 162, Boulder: 263–282.

Michaud, F.; Royer, J.Y.; Bourgois, J.; Dyment, J.; Calmus, T.; Bandy, W.; Sosson, M.; Mortera-Gutiérrez, C.; Sichler, B.; Rebolledo-Viera, M.; Pontoise, B. 2006. Oceanic-ridge subduction vs. slab break off: Plate tectonic evolution along the Baja California Sur continental margin since 15 Ma. Geology 34(1): 13–16. https://doi.org/10.1130/g22050.1

Middlemost, E.A.K. 1994. Naming materials in magma/igneous rock system. Earth-Sci. Rev. 37: 215–224.

Miyashiro, A. 1974. Volcanic rock series in island arcs and active continental margins. Am. J. Sci. 274: 321–355.

Molina-Garza, R.S.; Lawton, T.F.; Gudiño, J.R.B.; Sierra-Rojas, M.I.; Guadarrama, A.F.; Pindell, J. 2021b. Geochronology and correlation of the Todos Santos Group, western Veracruz and eastern Oaxaca States, Mexico: Implications for regional stratigraphic relations and the rift history of the Gulf of Mexico. In: Martens, U.C., Garza, R.S.M. (Eds), Southern and Central Mexico: Basement Framework, Tectonic Evolution, and Provenance of Mesozoic-Cenozoic Basins, Geological Society of America, v. 546: 0.

Nakamura, N. 1974. Determination of REE, Ba, Mg, Na and K in carbonaceous and ordinary chondrites. Geochim. Cosmochim. Acta 38: 757–773.

Nova, G.; Bayona, G.; Silva-Tamayo, J.; Cardona, A.; Rapalini, A.; Montaño, P.; Eisenhauer, A.; Dussan, K.; Valencia, V.; Ramírez, V.; Montes, C. 2019. Jurassic break-up of the Peri-Gondwanan margin in northern Colombia: Basin formation and implications for terrane transfer. J. South Am. Earth Sci. 89: 92–117.

O'Connor, J.T. 1965. A classification for quartz-rich igneous rocks based on feldspar ratios. U.S. Geol. Surv. Prof. Pap. B525: 79–84.

Palmer, B.A.; Shawkey, E.P. 2001. Lacustrine-fluvial transitions in a small intermountain valley, Eocene Callis volcanic field, Idaho. In: White, J.D.L.; Riggs, N.R. (Eds.), Volcaniclastic Sedimentation in Lacustrine Settings. Spec. Publ. Int. Assoc. Sedimentol. 30: 179–198.

Pearce, J.A.; Harris, N.W.; Tindle, A.G. 1984. Trace element discrimination diagrams for the tectonic interpretation of granitic rocks. J. Petrol. 25: 956–983.

Peccerillo, A.; Taylor, S.R. 1976. Geochemistry of Eocene calc-alkaline volcanic rocks from the Kastamonu area, Northern Turkey. Contrib. Mineral. Petrol. 58: 63–81.

Pindell, J.L.; Kennan, L. 2009. Tectonic evolution of the Gulf of Mexico, Caribbean and northern South America in the mantle reference frame: An update. In: James, K.; Lorente, M.A.; Pindell, J. (Eds.), The Origin and Evolution of the Caribbean Plate. Geol. Soc. Lond. Spec. Publ. 328: 1–55.

Pons, D. 1982. Paleobotanical and palynological studies of the Girón Formation (Middle Jurassic–Lower Cretaceous) in the Lebrija region, Santander Department, Colombia. C. R. Congr. Soc. Savantes 1 (107): 53–78.

Quandt, D.; Trumbull, R.B.; Altenberger, U.; Cardona, A.; Romer, R.L.; Bayona, G.; Guzmán, G. 2018. The geochemistry and geochronology of Early Jurassic igneous rocks from the Sierra Nevada de Santa Marta, NW Colombia, and tectono-magmatic implications. J. South Am. Earth Sci. 86: 216–230.

Ramirez, V.; Montes, C. 2019. Jurassic break-up of the Peri-Gondwanan margin in northern Colombia: Basin formation and implications for terrane transfer. J. South Am. Earth Sci. 89: 92–117.

Riel, N.; Jaillard, E.; Martelat, J.E.; Guillot, S.; Braun, J. 2018. Permian–Triassic Tethyan realm reorganization: Implications for the outward Pangea margin. J. South Am. Earth Sci. 81: 78–86.

Ríos, C.A.; García, C.A.; Takasu, A. 2003. Tectono-metamorphic evolution of the Silgará Formation metamorphic rocks in the southwestern Santander Massif, Colombian Andes. J. South Am. Earth Sci. 16: 133–154.

Rodríguez, G.; Arango, M.I.; Zapata, G.; Bermúdez, J.G. 2016. Catalog of lithostratigraphic units of Colombia, Saldaña Formation. Central and Eastern Cordilleras of Tolima, Huila, Cauca, and Putumayo. Serv. Geol. Colombiano: 91 p.

Rodríguez, G.; Arango, M.I.; Zapata, G.; Bermúdez, J.G. 2018. Petrotectonic characteristics, geochemistry, and U-Pb geochronology of Jurassic plutons in the Upper Magdalena Valley–Colombia: Implications on the evolution of magmatic arcs in the NW Andes. J. South Am. Earth Sci. 81: 10–30.

Rodríguez, G.; Correa, A.M.; Zapata, J.P.; Obando, G. 2019. Fragments of a Permian Arc on the Western Margin of the Neoproterozoic Basement of Colombia. In: Gómez-Tapias, J.; Mateu-Zabala, D. (Eds.), The Geology of Colombia. Servicio Geológico Colombiano 1 (10), Bogotá: 293–335.

Rodríguez, G.; Correa, A.M.; Zapata, G.; Arango, M.I.; Obando, G.; Zapata, J.P.; Bermúdez, J.G. 2020. Diverse Jurassic magmatic arcs of the Colombian Andes: Constraints from petrography, geochronology, and geochemistry. In: Gómez, J.; Pinilla–Pachón, A.O. (Eds.), The Geology of Colombia Volume 2: Mesozoic. Publicaciones Geológicas Especiales del Servicio Geológico Colombiano 36, Bogotá: 34–54.

Rojas-Parra, N.R.; Gómez-Isidro, S. 2007. Explanatory Report on Geological and Hydrogeological Research in the Guanentina Zone. Volume II. Geological and Hydrogeological Research Project in the Central Region of the Department of Santander. Specific UIS-INGEOMINAS Agreement 002/2005.

Ross, P.S.; Bédard, L.P. 2009. Magmatic affinity of modern and ancient subalkaline volcanic rocks determined from trace-element discriminant diagrams. Can. J. Earth Sci. 46: 823–839.

Royero, G.J.M.; Clavijo, J. 2001. Generalized Geological Map of Santander Department. Scale 1:400,000. INGEOMINAS Report: 92 p.

Schandl, E.S.; Gorton, M.P. 2002. Application of high field strength elements to discriminate tectonic settings in VMS environments. Econ. Geol. 97: 629–642.

Shaw, R.P.; Leal-Mejía, H.; Draper, J.C.M. 2019. Phanerozoic metallogeny in the Colombian Andes: a tectono-magmatic analysis in space and time. In: Cediel, F.; Shaw, R.P. (Eds.), Geology and Tectonics of Northwestern South America. Springer, Berlín: 411–549.

Schmid, R. 1981. Descriptive nomenclature and classification of pyroclastic deposits and fragments: recommendations of the IUGS Subcommission on the Systematics of Igneous Rocks. Geology 9: 41–43.

Schmitt, A.K.; Martín, A.; Weber, B.; Stockli, D.F.; Zou, H.; Shen, C.-C. 2013. Oceanic magmatism in sedimentary basins of the northern Gulf of California rift. GSA Bull. 125(11-12): 1833–1850. https://doi.org/10.1130/B30787.1

Spikings, R.; Cochrane, R.; Villagómez, D.; Van der Lelij, R.; Vallejo, C.; Winkler, W.; Beate, B. 2015. The geological history of northwestern South America, from Pangaea to the early collision of the Caribbean Large Igneous Province (290–75 Ma). Gondwana Res. 27 (1): 95–139.

Suárez, C.; Díaz, F. 2016. Petrographic and Stratigraphic Study of the Jordan Formation at its type locality on the southern scarp of the Mesa de Los Santos and Chicamocha River Canyon, Santander. Undergraduate Thesis, Universidad Industrial de Santander: 170 p.

Sun, S.S.; McDonough, W.F. 1989. Chemical and isotopic systematics of oceanic basalts: implications for mantle composition and processes. In: Saunders, A.D.; Norry, M.J. (Eds.), Magmatism in Ocean Basins. Spec. Publ. Geol. Soc. Lond. 42, London: 313–345.

Torres, T.; Philippe, M. 2002. New Species of Agathoxylon and Baieroxylon from the Lias of La Ligua (Chile) with an Evaluation of the Paleoxylological Record in the Jurassic of South America. Rev. Geol. Chile 29 (2): 151–165.

Toro-Toro, L.M.; Cardona-Ríos, J.J.; Moreno-Sánchez, M.; Gómez-Cruz, A. de J. 2021. Petrography and geochemistry of the pyroclastic and effusive rocks of the Bocas Formation (Upper Triassic-Lower Jurassic) and effusive rocks of the Nogontova Formation, Santander Massif, Colombia. Bol. Geol. 43 (1): 53–75.

Tschanz, C.M.; Marvin, R.F.; Cruz, J.; Mehnert, H.H.; Cebula, G.T. 1974. Geologic evolution of the Sierra Nevada de Santa Marta, Northeastern Colombia. Geol. Soc. Am. Bull. 85: 273–284.

Ureña, C.L.; Zuluaga, C.A. 2011. Petrografía del Neis de Bucaramanga en cercanías a Cepitá, Berlín y Vetas (Santander). Geol. Colombiana (Esp. Ed.) 36 (1): 37–56.

Van Der Lelij, R.; Spikings, R.; Ulianov, A.; Chiaradia, M.; Mora, A. 2016. Palaeozoic to Early Jurassic history of the northwestern corner of Gondwana, and implications for the evolution of the Iapetus, Rheic and Pacific Oceans. Gondwana Res. 31: 271–294.

Walker, G.P. 1983. Ignimbrite types and ignimbrite problems. J. Volcanol. Geotherm. Res. 17 (1–4): 65–88.

Ward, D.E.; Goldsmith, R.; Cruz, B.J.; Jaramillo, C.L.; Restrepo, H. 1973. Geology of Quadrangles H-12, Bucaramanga, and H-13, Pamplona, Santander Department. U.S. Geol. Surv. - INGEOMINAS. Bol. Geol. XXI (1–3): 1–132.

Winchester, J.A.; Floyd, P.A. 1977. Geochemical discrimination of different magma series and their differentiation products using immobile elements. Chem. Geol. 20: 325–343.

Ziegler, P.A.; Cloetingh, S. 2004. Dynamic processes controlling evolution of rifted basins. Earth Sci. Rev. 64(1–2): 1-50. https://doi.org/10.1016/S0012-8252(03)00041-2

Zuluaga, C.A.; Pinilla, A.; Mann, P. 2015. Jurassic silicic volcanism and associated Continental-arc Basin in northwestern Colombia (southern boundary of the Caribbean plate). In: Bartolini, C.; Mann, P. (Eds.), Petroleum Geology and Potential of the Colombian Caribbean Margin. Am. Assoc. Petrol. Geol. Mem. 108, Tulsa: 137–160.

Zuluaga, C.A.; López, J.A. 2019. Ordovician orogeny and Jurassic low-lying orogen in the Santander Massif, northern Andes, Colombia. In: Cediel, F.; Shaw, R.P. (Eds.), Geology and Tectonics of Northwestern South America. Springer Nature, Cham: 195–250.